(12)

RADC-TR-77-261
Final Technical Report
August 1977

WIDEBAND DIGITAL TRANSMITTER/RECEIVER

TRW Defense and Space Systems

DDC

SEP 26 1977

C

Approved for public release; distribution unlimted.

ROME AIR DEVELOPMENT CENTER
Air Force Systems Command
Griffiss Air Force Base, New York 13441

This report has been reviewed by the RADC Information Office (OI) and is releasable to the National Technical Information Service (NTIS). At NTIS it will be releasable to the general public, including foreign nations.

This report has been reviewed and approved for publication.

APPROVED: *[signature: Lewis A. Javarone]*

LEWIS A. JAVARONE
Project Engineer

APPROVED: *[signature: Fred I. Diamond]*

FRED I. DIAMOND
Technical Director
Communications and Control Division

FOR THE COMMANDER: *[signature: John P. Huss]*

JOHN P. HUSS
Acting Chief, Plans Office
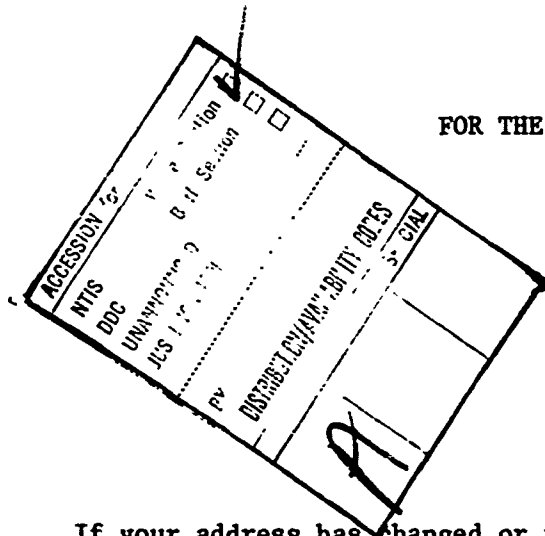
If your address has changed or if you wish to be removed from the RADC mailing list, or if the addressee is no longer employed by your organization, please notify RADC (DAP) Griffiss AFB NY 13441. This will assist us in maintaining a current mailing list.

Do not return this copy. Retain or destroy.

SECURITY CLASSIFICATION OF THIS PAGE (When Data Entered)

REPORT DOCUMENTATION PAGE	READ INSTRUCTIONS BEFORE COMPLETING FORM

1. REPORT NUMBER	2. GOVT ACCESSION NO.	3. RECIPIENT'S CATALOG NUMBER
RADC-TR-77-261		

4. TITLE (and Subtitle)	5. TYPE OF REPORT & PERIOD COVERED
WIDEBAND DIGITAL TRANSMITTER/RECEIVER	Final Technical Report. May 1976 – March 1977
	6. PERFORMING ORG. REPORT NUMBER N/A

7. AUTHOR(s)	8. CONTRACT OR GRANT NUMBER(s)
Donald L. Lochhead	F30602-76-C-0278

9. PERFORMING ORGANIZATION NAME AND ADDRESS	10. PROGRAM ELEMENT, PROJECT, TASK AREA & WORK UNIT NUMBERS
TRW Defense & Space Systems 1 Space Park Redondo Beach CA 90278	62702F 65231102

11. CONTROLLING OFFICE NAME AND ADDRESS	12. REPORT DATE
Rome Air Development Center (DCCT) Griffiss AFB NY 13441	August 1977
	13. NUMBER OF PAGES 48

14. MONITORING AGENCY NAME & ADDRESS(If different from Controlling Office)	15. SECURITY CLASS. (of this report)
Same	UNCLASSIFIED
	15a. DECLASSIFICATION/DOWNGRADING SCHEDULE N/A

16. DISTRIBUTION STATEMENT (of this Report)

Approved for public release; distribution unlimited.

17. DISTRIBUTION STATEMENT (of the abstract entered in Block 20, if different from Report)

Same

18. SUPPLEMENTARY NOTES

RADC Project Engineer:
Lewis A. Javarone (DCCT)

19. KEY WORDS (Continue on reverse side if necessary and identify by block number)

MSK Modulation
QPSK Modulation
Ka-Band Link
Bit Error Rate
500 Mbps Digital Link

20. ABSTRACT (Continue on reverse side if necessary and identify by block number)

A laboratory test was conducted to evaluate the bit error rate performance of a 500 Mbps Ka-band demonstration link. Three types of modulation were evaluated; MSK, coherent QPSK, and differentially coherent QPSK. Theoretical calculations which predicted that MSK would be superior to both forms of QPSK were confirmed. Complete performance data including BER, waveform photographs, and spectrum occupancy is presented.

DD FORM 1 JAN 73 1473 EDITION OF 1 NOV 65 IS OBSOLETE

TABLE OF CONTENTS

LIST OF ILLUSTRATIONS

LIST OF ILLUSTRATIONS (Continued)

LIST OF TABLES

EVALUATION

New techniques for achieving improved bit error rates in high speed digital links are of continuing interest. One such new technique is MSK modulation.

The purpose of this study was to determine the bit error rate performance of both MSK and QPSK modulated signals. The tests were designed to evaluate the suitability of each type of modulation for use in a 500 Mbps Ka-band terrestrial link.

The use of MSK and QPSK, in a 500 Mbps Ka-band link has therefore, been demonstrated and the predicted superior BER of MSK compared to QPSK has been confirmed.

LEWIS A. JAVARONE
Project Engineer

SECTION I
INTRODUCTION AND SUMMARY

This final report describes the results of a test program performed by TRW Defense and Space Systems under contract No. F30602-76-C-0278, Wideband Digital Transmitter/ Receiver, for the Air Force Systems Command, Rome Air Development Center. The period of performance was 15 May 1976 through 25 March 1977. The purpose of the program was to demonstrate the feasibility of a 500 Mbps digital link operating in the 36 to 38.6 GHz band.

Military requirements for digital communication links have steadily increased in the previous years and are projected to continue doing so. In support of this prediction is the continuing trend to upgrade existing systems and to configure new ones using digital modulation techniques. Future communication systems in the next decade are predicted to become fully digital to take advantage of less cumulative noise degradation, greater flexibility of multiplexing, and adaptability to secure encryption.

The increasing amount of communications traffic is rapidly utilizing all of the available bandwidth in the current frequency bands up through Ku-band. For this reason future communication links are being configured to operate at higher and higher frequencies. The 36 to 38.6 GHz band is currently being evaluated for digital use because it offers the required bandwidths for high data rate links.

This program demonstrated the use of three different types of modulation for a 500 Mbps Ka-band link. The three types of modulation evaluated were coherent quadriphase shift keyed (QPSK), differentially coherent QPSK, and minimum shift keyed (MSK). To perform this task, two sets of equipment were assembled. The first was a digital terminal which served as both the data transmitter and receiver. The second was a Ka-band demonstration link which simulated the degradation to the modulated signal which occurs when the signal is transmitted through an actual 10 km Ka-band link.

The key parameter used to establish the performance of the link using each of the three modulation formats was the bit error rate (BER). The testing was performed in two phases. During the first phase, the BER of the digital terminal alone was measured. The testing was then repeated by transmitting the modulated signal through the demonstration link. The results of these tests confirmed the predictions that MSK would operate with the lowest overall BER and that of the two forms of QPSK, coherent would be superior.

This investigation provided some of the basic data necessary to specify a modulation type for a Ka-band 500 Mbps data link. The relative BER performance of the three candidate modulation types has been established. For systems in which the lowest possible BER is required, MSK modulation should be used. For links with less stringent BER requirements, coherent QPSK would be optimum. And finally, for systems with relaxed BER requirements, differentially coherent QPSK is a low cost alternative.

1

SECTION II
PROGRAM TEST RESULTS

The purpose of this program was to characterize the bit error rate (BER) performance of a Ka-band link operating at a data rate of 500 Mbps. Three different types of modulation were evaluated: minimum shift keying (MSK), coherent quadriphase shift keying (QPSK), and differentially coherent QPSK.

To perform this task two sets of equipment were utilized. The first is a high data rate digital terminal consisting of QPSK and MSK modulators, an IF noise source, demodulator, bit synchronizer, data generator, and bit error rate counter. The second set of equipment is the Ka-band demonstration link and consists of an S to Ka-band upconverter, a Ka-band avalanche diode amplifier (ADA), a Ka to S-band downconverter, and the appropriate local oscillators. This equipment is detailed in Section 3.

The testing was conducted in two phases. The first phase characterized the digital terminal alone and the second phase characterized the combined terminal and demonstration link. This sequence of testing was followed to separate the degradation resulting from the modulator, demodulator, and bit synchronizer from the degradation due to the distortion in the link. The results of these tests and the computer simulated error rates are summarized in Table 1. At a BER of 1×10^{-6}, the differential degradation introduced by the Ka-band link was 0.2 dB for MSK, 0.7 dB for coherent QPSK, and 0.9 dB for differentially coherent QPSK. The simulated degradation for MSK was 0.4 dB and 0.8 dB for both forms of QPSK.

TABLE 1. BER PERFORMANCE SUMMARY

Configuration	BER Degradation at Error Rate of 1×10^{-6}		
	MSK	Coherent QPSK	Differentially Coherent QPSK
IF back-to-back	0.5 dB	1.0 dB	3.0 dB
Ka-band demonstration link — measured	0.8 dB	1.7 dB	3.9 dB
Differential degradation	0.2 dB	0.7 dB	0.9 dB
Computer simulated differential degradation	0.4 dB	0.8 dB	0.8 dB

Prior to performing the BER measurements, each of the components used in assembling the Ka-band demonstration link was completely characterized. Single-tone swept gain and phase vs frequency measurements were obtained for a range of input drive levels about nominal power. This characterization was then analyzed to determine the amplitude flatness, phase nonlinearity, AM/AM, and AM/PM for each component. The results of these tests and analysis are summarized in Table 2.

TABLE 2. LINK DISTORTION SUMMARY

Component	Distortion				
	Amplitude Flatness (dB)		Phase (deg) Nonlinearity	AM/AM	AM/PM
	$f_0 \pm 150$ MHz	$f_0 \pm 300$ MHz	$f_0 \pm 150$ MHz	(dB/dB)	(deg/dB)
Complete link	±0.5	±1.7	±5.0	0.1	1.5
Upconverter/downconverter	±0.4	±0.6	±1.5	0.9	0.5
Avalanche diode amplifier	±0.25	±0.65	±7.0	0.1	1.0
Bandpass filter	±0.1	±1.5	±3.5	—	—

2.1 LINK CHARACTERIZATION

The swept phase and gain characteristics for each major component used to assemble the Ka-band demonstration link were measured using a manual network analyzer. Each component was measured at its nominal input power and at several levels above and below nominal. By necessity, these characteristics were measured from S-band to S-band. Hence, the ADA measurements include a prior upconverter and subsequent downconverter. However, the input level to the ADA was varied by a wideband attenuator between the upconverter and the ADA so that the upconverter characteristic remains constant and may be subtracted from the total response to obtain the response of the ADA alone.

For the purpose of characterization, the Ka-band demonstration link is considered to consist of three basic subassemblies: an S-band to Ka-band to S-band upconverter/downconverter, a Ka-band avalanche diode amplifier, and an S-band bandpass filter. Figures 1 through 6 show the swept phase and gain for each of these subassemblies. The upconverter/downconverter and the bandpass filter were individually characterized, and the ADA was characterized using the upconverter/downconverter as previously explained. In addition, the response of the complete link is shown in Figure 7. The analysis of all of these curves was summarized in Table 2.

3
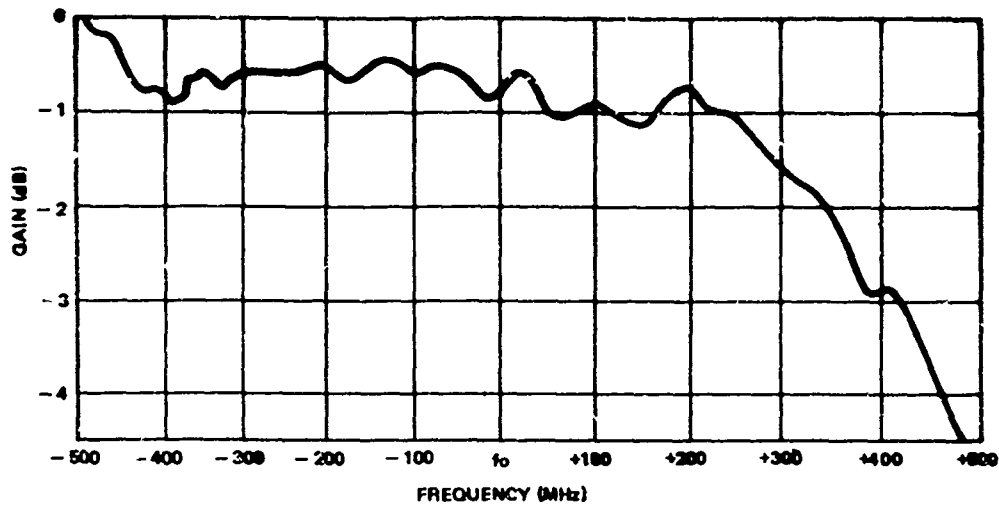
Figure 1. Ka-Band Upconverter/Downconverter Gain Variation
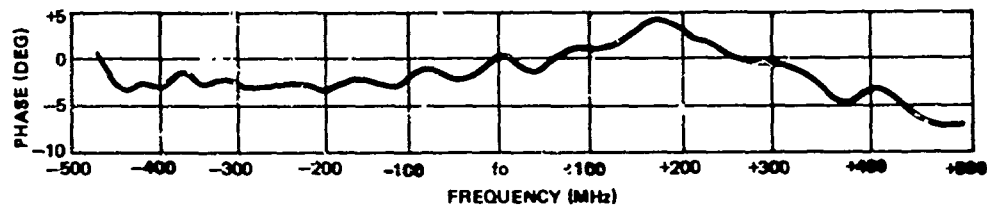
Figure 2. Ka-Band Upconverter/Downconverter Phase Nonlinearity
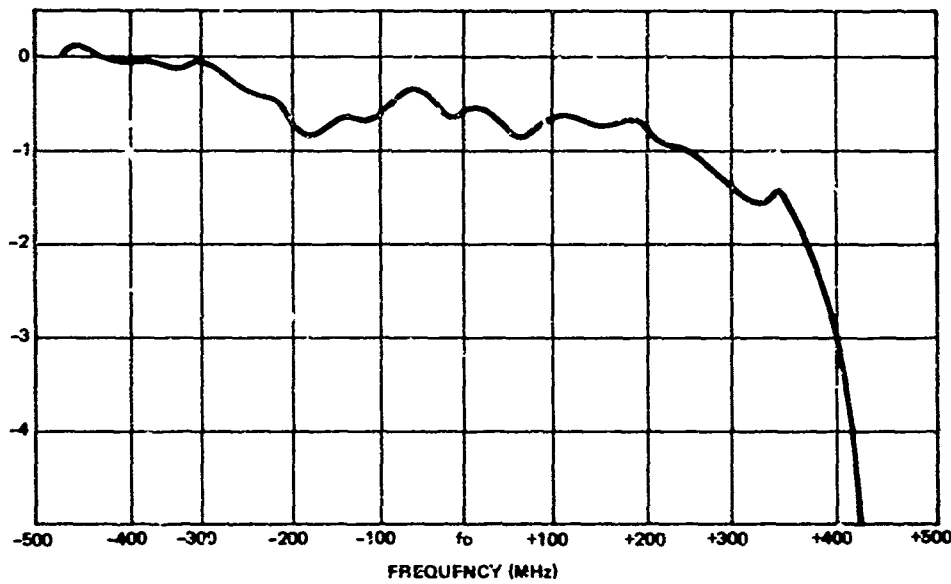
Figure 3. Ka-Band ADA Gain Variation

4
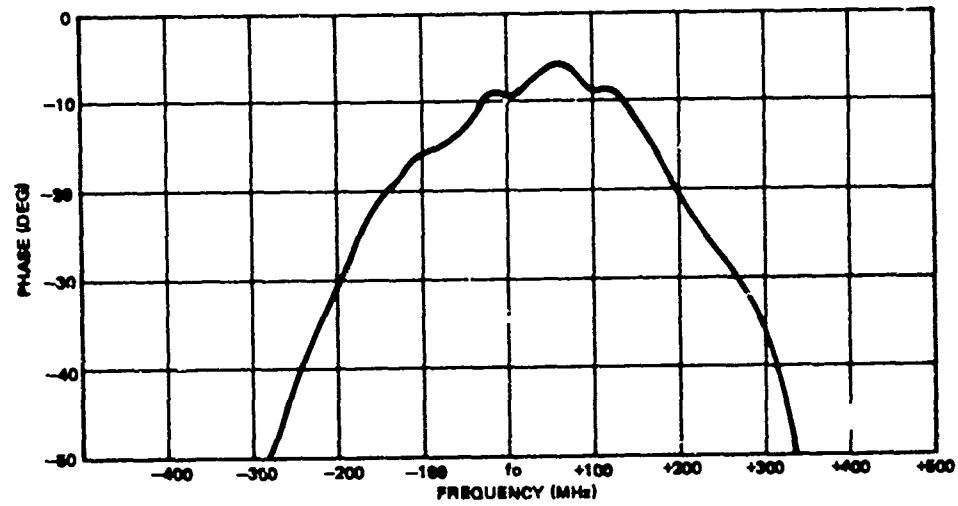
Figure 4. Ka-Band ADA Phase Nonlinearity
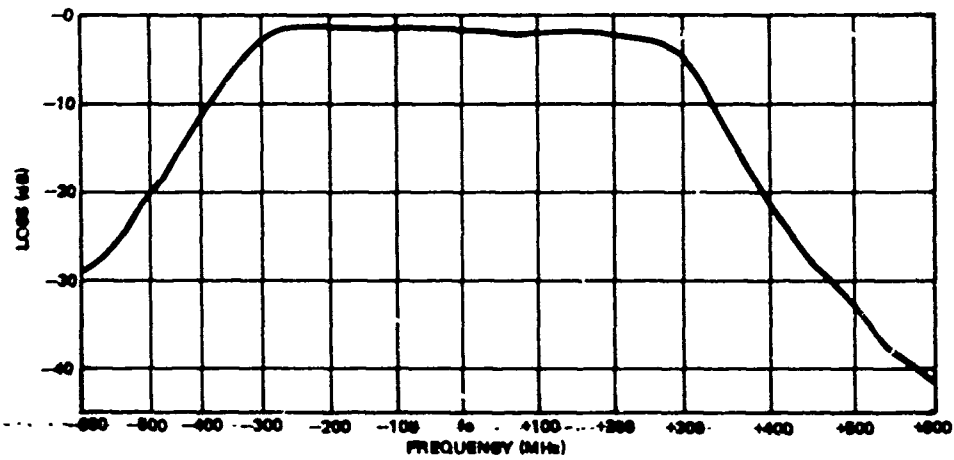
Figure 5. Bandpass Filter Insertion Loss
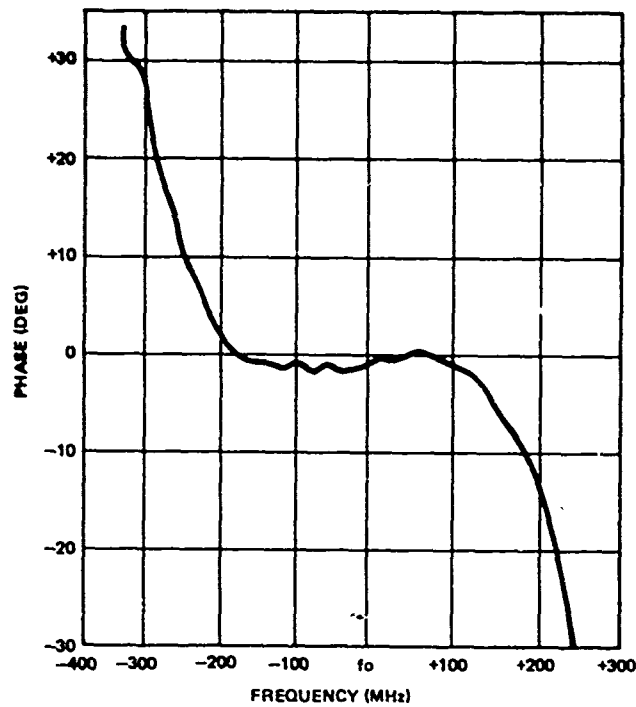
Figure 6. Bandpass Filter
Phase Nonlinearity

5
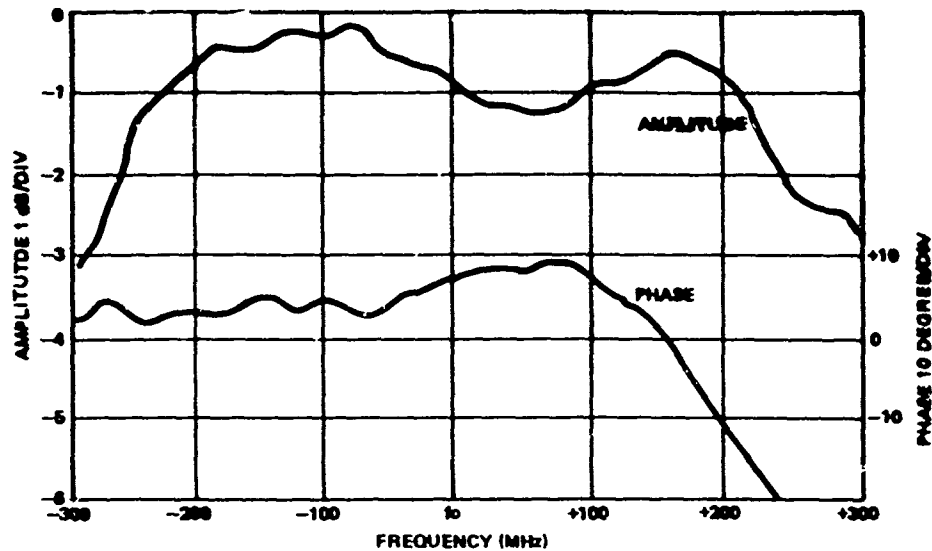
Figure 7. Ka-Band Demonstration Link Total Passband Response

2.2 DIGITAL TERMINAL CHARACTERIZATION

The digital terminal equipment was extensively characterized to determine the basic BER of the modulated signal prior to being transmitted through the demonstration link. The testing was performed in accordance with the program test plan which is included as an appendix of this report. In addition to performing BER measurements, time and frequency domain photographs were taken of the baseband, modulated, and demodulated signals. These photos were analyzed to determine the si.. ..transition time, asymmetry, and spectrum occupancy. This series of tests was performed three times, once for each form of modulation/demodulation evaluated. The following sections describe these tests.

2.2.1 Digital Terminal Tests/MSK Modulation

The digital terminal was configured to characterize the MSK modulator as shown in Figure 8. Table 3 summarizes the results of these measurements. Testing included BER measurements and the recording of the modulator waveforms at all of the major interfaces in the system.
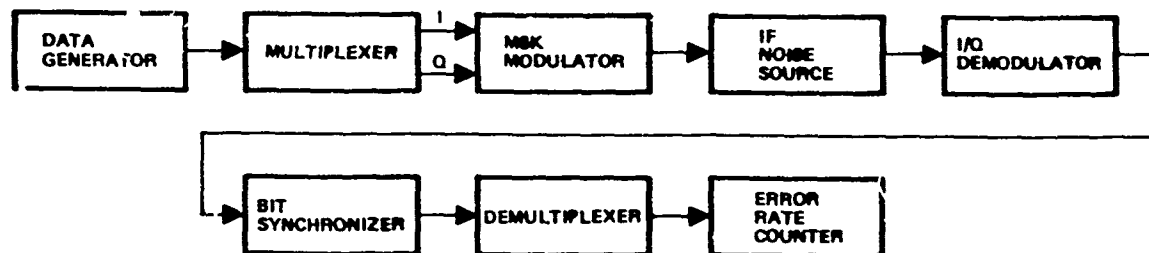
Figure 8. MSK Digital Terminal Test Configuration

TABLE 3. MSK DIGITAL TERMINAL TEST RESULT SUMMARY

Parameter	Performance
BER degradation at 1×10^{-6}	0.6 dB
Data asymmetry	±200 psec

BER Tests

The BER performance of the MSK modulator was measured over an E_b/N_o range of 8 to 12 dB. This was sufficient to vary the resulting error rate from $>10^{-4}$ to $<10^{-7}$. The measured degradation from theoretical was a constant 0.6 dB over the full E_b/N_o range. The complete BER curve is shown in Figure 9. The fact that the error rate did not flair at high E_b/N_o values indicates that the complete system was properly operating and that there were no anomalous sources of errors such as phase noise or improper timing in the bit synchronizer.
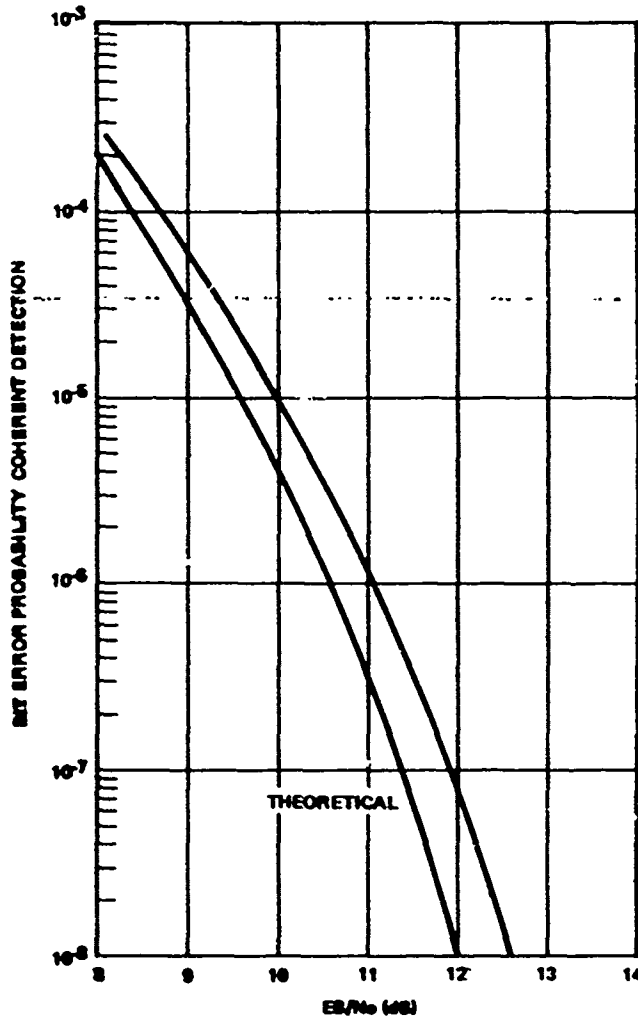
Figure 9. MSK Digital Terminal BER Performance

7

Spectrum Occupancy

The spectrum occupancy of the MSK modulated signal was determined using a manual spectrum analyzer. Figure 10 shows the RF output spectrum of the modulator. The multiple nulls in the spectrum are due to multiplexing which occurs in the PRN sequence generator and the skew between the I and Q channels. The first null in the MSK spectrum occurs at 1.35 x the baud rate. Therefore, the first nulls occur at ±340 MHz (1.35 x 250 MHz), which is clearly seen in the photograph. In addition, the photograph shows that all of the modulated energy outside the ±300 MHz link bandwidth is down by >25 dB with respect to the maximum in-band level.
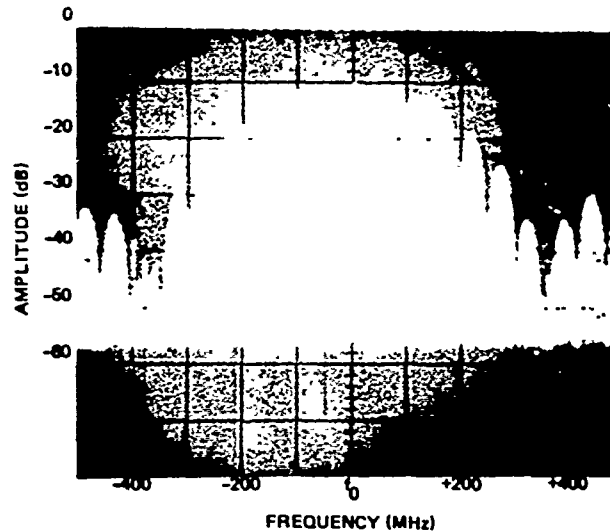
Figure 10. MSK Modulator Output Spectrum

Demodulated Waveforms

The waveforms at the output of the demodulator were recorded and analyzed to determine the data asymmetry and overall quality of the signal. These photographs are shown in Figure 11. The overview photograph shows 25 consecutive bits of the I and Q channels, from which it is possible to see the cosinesoidal pulse shape of the demodulated MSK waveform. The second photograph is an eye pattern and is useful in determining the asymmetry of the demodulated signal. The pattern is the sum of all of the bits in the 127-bit PRN sequence. The width of the pattern at the zero crossing represents the total asymmetry throughout the entire sequence and includes the effects of any pattern sensitivity. For the MSK signal, the demodulated asymmetry is ±200 psec.

2.2.2 Digital Terminal Tests/Coherent QPSK Modulation

The second terminal configuration that was evaluated was coherent QPSK. The block diagram of the terminal for these tests is shown in Figure 12. The results of these tests are summarized in Table 4. Testing included BER measurements and the recording of the modulator waveforms at all of the major interfaces in the system.

TABLE 4. QPSK DIGITAL TERMINAL TEST RESULT SUMMARY

Parameter	Performance
BER degradation at 1×10^{-6}	1.0 dB
Data transition time	500 psec
Data asymmetry	±250 psec
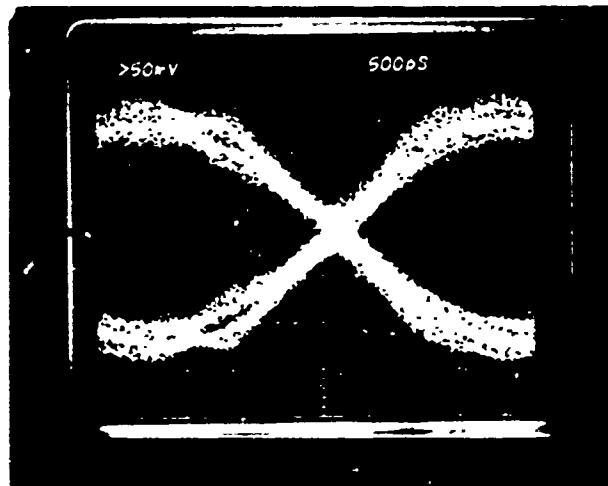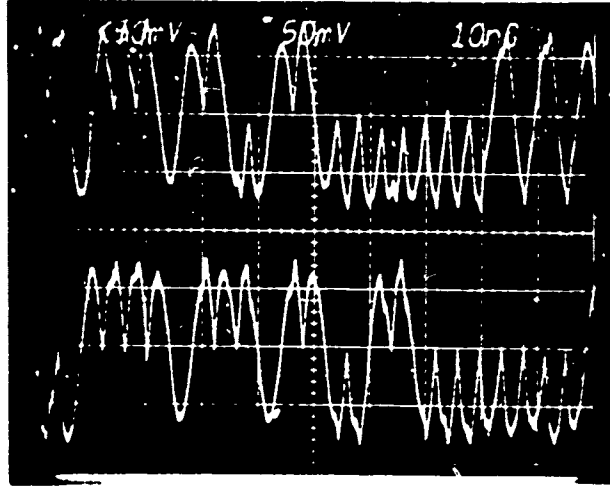
b) Demodulated MSK Signal Eye Pattern

Figure 11. Digital Terminal Waveforms
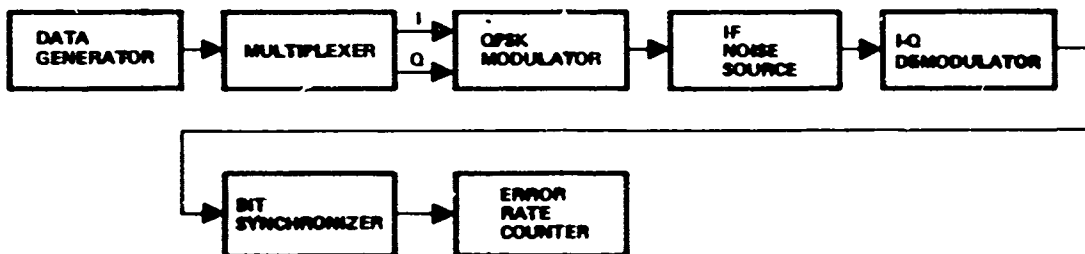
Figure 12. Coherent QPSK Digital Terminal Test Configuration

9

BER Tests

The BER performance of the QPSK modulator, as shown in Figure 13, was measured over an E_b/N_0 range of 8 to 14 dB. This range was sufficient to vary the resulting error rate from $>10^{-4}$ to $<10^{-7}$. The measured degradation from theoretical was 1.0 dB at an error probability of 1×10^{-6} and increased to 1.4 dB at an error probability of 1×10^{-9}. The slight increase in error rate is due to the finite imperfections in the bit synchronizer timing.
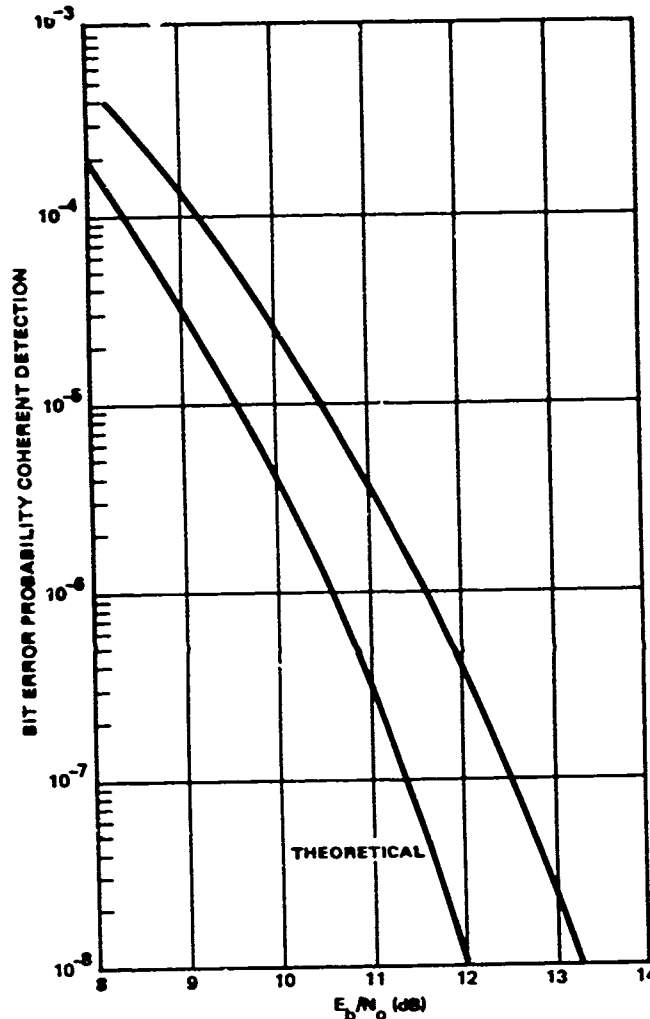

Figure 13. Coherent QPSK Digital Terminal BER Perform

Spectrum Occupancy

The spectrum occupancy of the QPSK modulated signal was determined using a manual spectrum analyzer. Figure 14 shows the output spectrum of the modulator. The first nulls of the spectrum envelope are at ±250 MHz (1 x baudrate). The extra nulls in the spectrum are due to the correlation between the I and Q channels. From the photo it can be seen that there is still significant energy outside the ±300 MHz link bandwidth. The maximum level outside the band is 15 dB below the in-band peak compared to >25 dB for MSK.

10
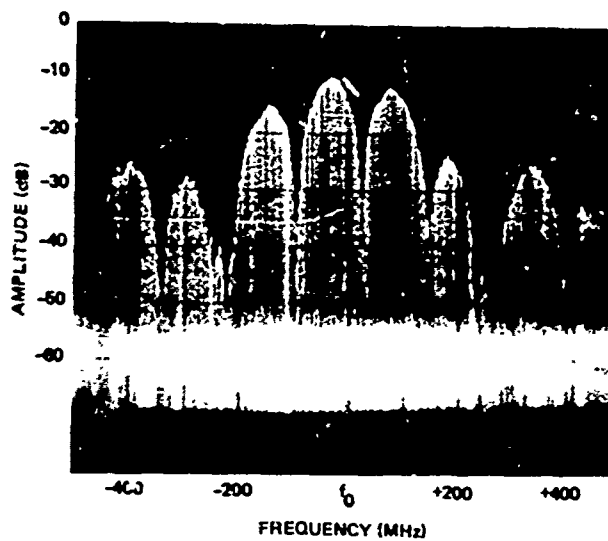
Figure 14. Coherent QPSK Modulator Output Spectrum

Demodulated Waveforms

The waveforms at the output of the demodulator were recorded and analyzed to determine the 10 to 90% transition time, data asymmetry, and overall quality of the signal. These photographs are shown in Figure 15. The overview photograph shows 25 consecutive bits of the I and Q channels. The transition time photo is a double exposure of both the rise and fall time of a typical bit. The typical demodulated 10 to 90% transition time was 700 psec. Assuming equal contributions for both the modulator and demodulator and that the measured transition time is the rms value of the two, the calculated modulator transition time is 500 psec. The final photograph is the eye pattern for the demodulated QPSK signal. Analysis of this photo indicates that the maximum asymmetry throughout the code is ±250 psec.

2.2.3 Digital Terminal Tests/Differentially Coherent QPSK Modulation

The third and final terminal configuration evaluated was differentially coherent QPSK. The block diagram of the terminal for these tests is shown in Figure 16. The results of these tests are summarized in Table 5. Testing included BER measurements and the recording of the modulator waveforms at all of the major interfaces in the system.

TABLE 5. DIFFERENTIALLY COHERENT QPSK DIGITAL
TERMINAL PERFORMANCE SUMMARY

Parameter	Performance
BER degradation at 1×10^{-6}	3.0 dB
Data transition time	330 psec
Data asymmetry	±250 psec

11
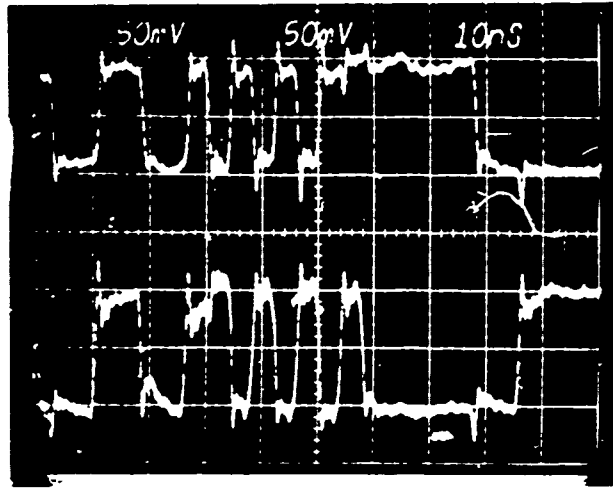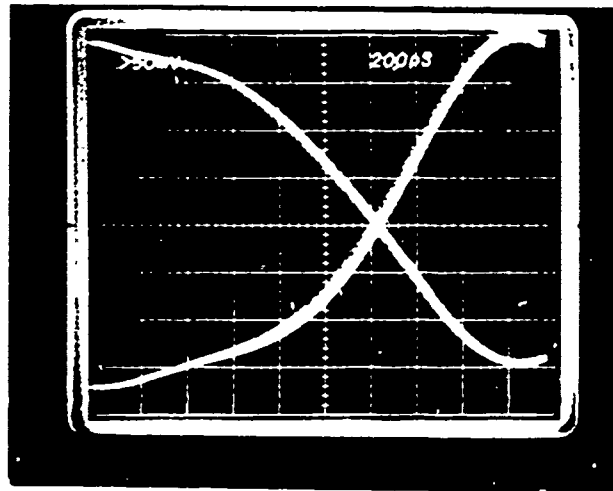
a) QPSK Waveforms

b) QPSK Rise and Fall Times
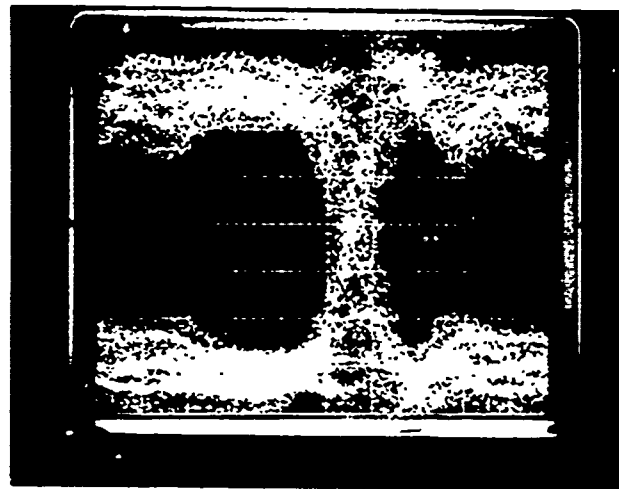
c) QPSK Signal Eye Pattern

Figure 15. Digital Terminal Demodulatcd Waveforms

12
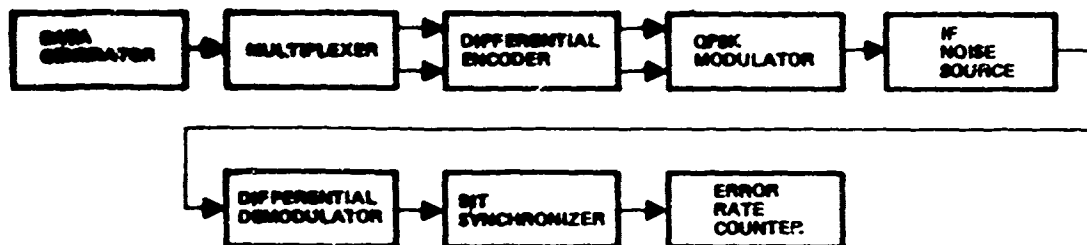
Figure 16. Differentially Coherent QPSK Digital Terminal Test Configuration

BER Tests

The BER performance of the differentially coherent QPSK modulator as shown in Figure 17 was measured over an E_b/N_o range of 13 to 18 dB   This range was sufficient to vary the resulting error rate from $>10^{-4}$ to $<10^{-7}$. The measured degradation from theoretical was 3.0 dB at an error probability of 1×10^{-6} and increased to 3.9 dB at an error probability of 1×10^{-8}. This represents a significant flare in the error rate and indicates the generally lower level of performance of the differentially coherent system. It should be noted that the theoretical curve for differential QPSK is shifted to the right by approximately 2.4 dB compared to the theoretical curve for coherent QPSK. This shift is due to the effects of demodulating the signal with another noisy signal (a delayed version of itself) rather than with a noise free local oscillator.
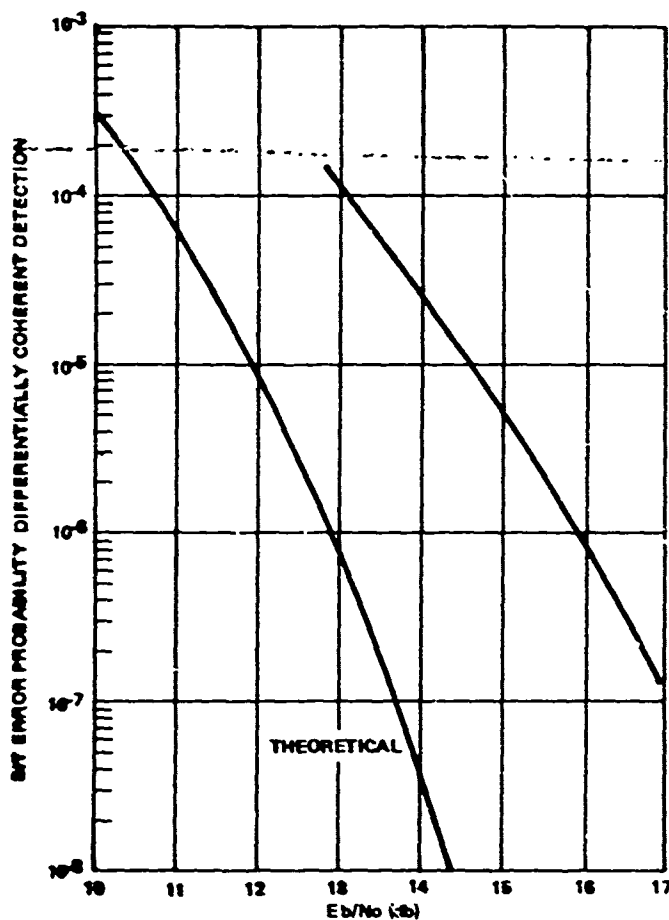
Figure 17. Differentially Coherent QPSK Digital Terminal BER Performance

13

Spectrum Occupancy

The spectrum occupancy of the differentially coherent QPSK signal was determined using a manual spectrum analyzer. Figure 18 shows the RF output spectrum of the modulator. The spectral line spacing for the differentially encoded QPSK is 492 kHz vs 1.968 MHz for QPSK and MSK tests. This is because the differential encoding increases the PRN code length from its normal value of 127 bits by a factor of 4 to 508 bits. The differential encoding does not affect the other spectral occupancy parameters. The first nulls for the spectrum remain at ±250 MHz (1 x the baud rate). As with coherent QPSK, there is significant energy outside the ±300 MHz link bandwidth.
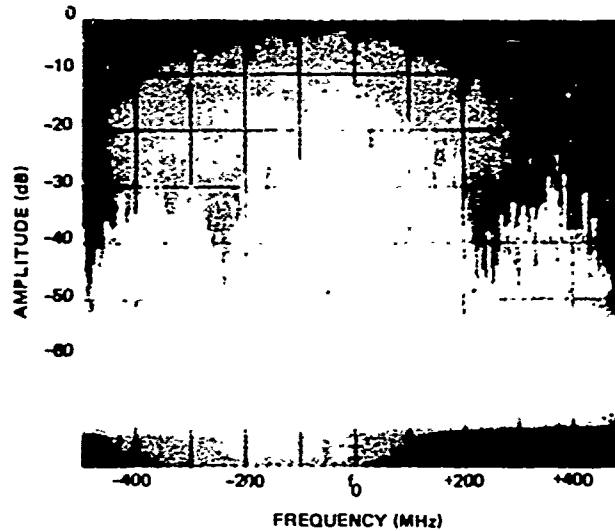
Figure 18. Differentially Coherent QPSK Modulator Output Spectrum

Demodulated Waveforms

The waveforms at the output of the demodulator were recorded and analyzed to determine the 10 to 90% transition time, data asymmetry, and overall quality of the signal. These photographs are shown in Figure 19. The overview photograph shows 25 consecutive bits of the I and Q channels. From the photo, it is evident that there is considerably more distortion on the demodulated waveform compared to coherent QPSK (refer to Figure 15a), particularly in the sequence of seven consecutive 1's. This higher level of distortion is due to the fact that the power level of both input signals to the demodulator phase detectors are continuously changing compared to coherent QPSK which utilizes a constant amplitude local oscillator.

The transition time of the demodulated signal was improved by the differential encoding at the expense of significant overshoot in the transition. The calculated value assuming a demodulator rise time of 500 psec was 330 psec. The improvement in risetime is due to the fact that both inputs to the demodulator are simultaneously changing and result in a higher dv/dt at the phase detector. The asymmetry of the differentially encoded signal was degraded. Analysis of the demodulated eye pattern shows the asymmetry to be ±350 psec compared to ±250 psec for coherent QPSK. This effect is also the consequence of not using a stable local oscillator to demodulate the signal.

14
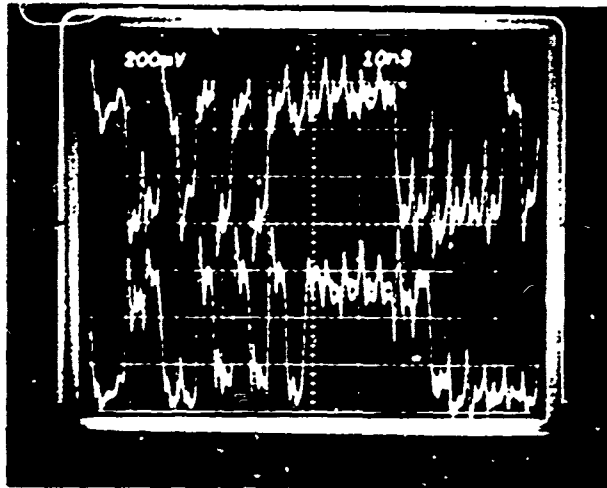
a) Differentially Coherent QPSK Waveforms
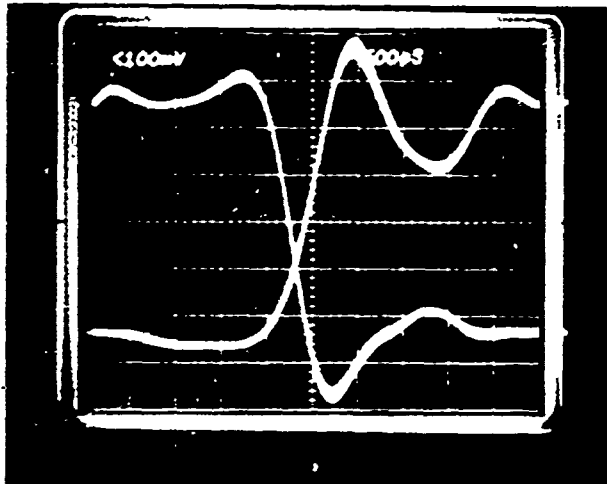
b) Differentially Coherent QPSK Rise and Fall Times
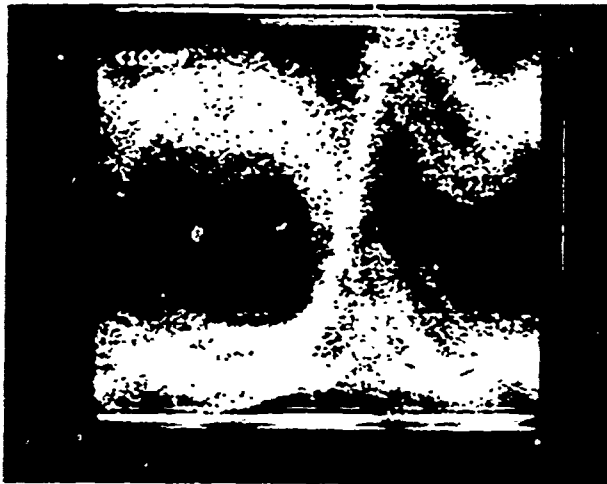
c) Differentially Coherent QPSK Signal
Eye Pattern

Figure 19. Digital Terminal Demodulated Waveforms

15

2.3 COMBINED DIGITAL TERMINAL/Ka-BAND LINK TESTS

The final phase of this program was the testing of the complete system. This series of tests served two purposes: first to determine the BER of the total system, and second, when the results of these tests are compared to the performance of just the digital terminal, it is possible to determine the incremental degradation intro- duced by the Ka-band link. The same basic test philosophy employed to characterize the digital terminal alone was followed in this set of tests. The testing was per- formed in accordance with the program test plan (refer to the appendix). In addition to performing BER measurements, time and frequency domain photographs were taken of the modulated and demodulated signals. These photos were analyzed to determine the signal transition time, asymmetry, and spectrum occupancy. This series of tests was performed three times, once for each form of modulation/demodulation being evaluated. The follow- ing sections describe these tests.

2.3.1 Demonstration Link Tests/MSK Modulation

The digital terminal and demonstration link were configured as shown in Figure 20 to characterize the BER of the system using MSK modulation. The results of the testing are summarized in Table 6. Testing included BER measurements and photographing of the modulated and demodulated waveforms.

TABLE 6. MSK Ka-BAND DEMONSTRATION LINK
PERFORMANCE SUMMARY

Parameter	Performance
BER degradation at 1×10^{-6}	0.8 dB
Data asymmetry	±200 psec
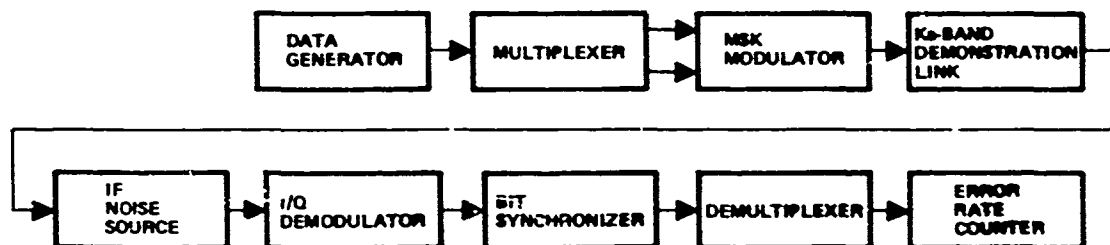
Figure 20. MSK Demonstration Link Test Configuration

BER Tests

The BER performance of the Ka-band link using MSK modulation was measured over an E_b/N_o range of 8 to 13 dB. This was sufficient to vary the resulting bit error rate from $>10^{-4}$ to $<10^{-7}$. The measured degradation from theoretical was 0.8 dB at an error rate of 10^{-6}, and increased to 1.0 dB at 5×10^{-8}. The slight increase in BER is due to the effects of noise in the Ka-band link. The complete BER curve is shown in Figure 21.
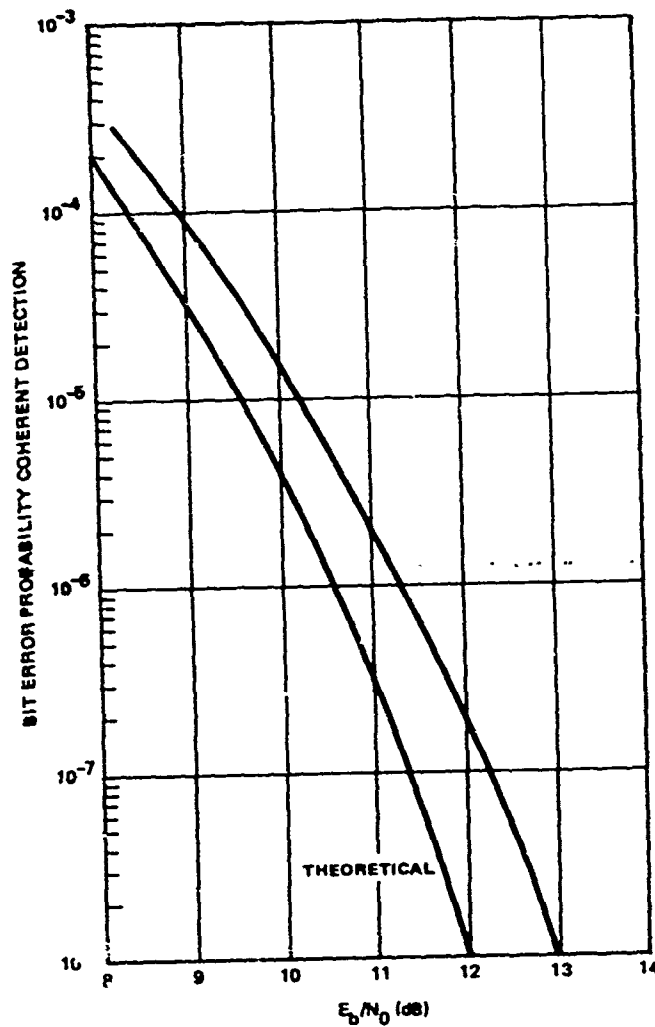
Figure 21. Ka-Band Demonstration Link MSK BER Performance

The net increase in system BER due to the Ka-band link was only 0.2 dB. Although this result is low it is consistent with the known properties of MSK. Two factors contribute to the excellent performance: first, the link bandwidth is sufficient to transmit >99% of the MSK signal energy, and second, the phase and amplitude distortions in the link passband is minimal.

17

The demonstration link was configured so that it was possible to bypass the ADA. This made it possible to measure the performance of the link with and without the ADA. The result of the test was that the ADA improved the BER of the system by 0.15 dB. This result is consistent with the computer simulations of the link. The improvement is due to the saturation in the ADA which reduces the residual AM on the MSK signal and therefore improves the BER. The remainder of the link components are all operated in a linear mode, and therefore do not contribute to this effect.

Utilization of saturated amplifiers is a common technique in phase modulated systems and must be carefully controlled to achieve the desired performance improvement. There are two key parameters to control when using saturated amplifiers: passband shape variation vs input level, and AM/PM. The Ka-band ADA utilized in these tests was carefully aligned to optimize both of these parameters. In addition, these parameters must be controlled over the full bandwidth of the modulated signal. As will be discussed in Section 2.3.2, in the case of the QPSK testing, the saturated ADA degraded the link performance. This was because the bandwidth of the QPSK modulated signal exceeded the bandwidth of the ADA. Thus, the signal suffered a net degradation when transmitted through the ADA.

Spectrum Occupancy

A photograph of the spectrum occupancy of the MSK waveform after being transmitted through the complete Ka-band demonstration link is shown in Figure 22. Compared to the MSK spectrum recorded directly at the output of the modulator (refer to Figure 10), there is very little visible distortion to the modulated spectrum. The only effect was a slight distortion in the top of each lobe. The one result of being transmitted through the link that is quite evident is the bandlimiting which has occurred. There is no detectable signal energy outside the ±300 MHz link bandwidth.
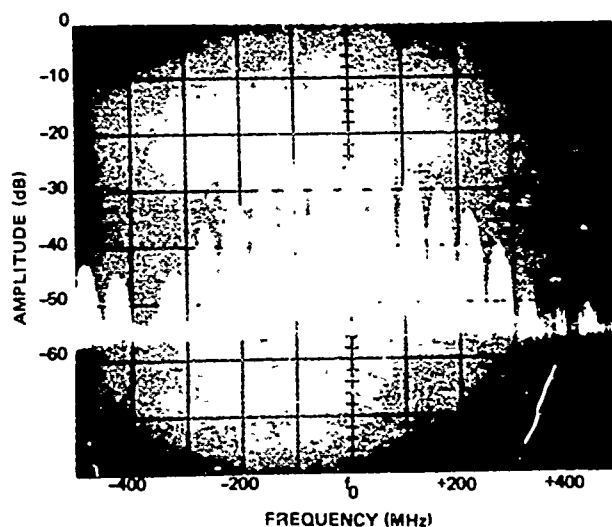
Figure 22.   MSK Modulated Signal Spectrum at Output of
Ka-Band Demonstration Link

18

Demodulated Waveforms

The waveforms at the output of the demodulator were recorded and analyzed to determine the data asymmetry and overall quality of the signal. These photographs are shown in Figure 23. The overview photograph shows 25 consecutive bits of the I and Q channels. This photo shows the effect of the link bandlimiting on the demodulated waveform. Each pulse should return to the 50% point, but the bandlimiting prevents this. This form of degradation is not particularly severe because it does not significantly affect the peak value of the signal after it has been integrated prior to the decision process.

The second photograph is the demodulated eye pattern of the signal. Analysis of this photograph indicates that the asymmetry is ±200 psec, which is unchanged from the value measured directly at the output of the modulator.
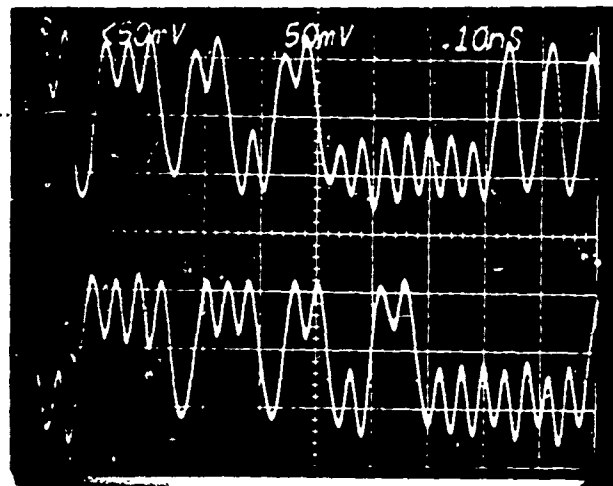
a) MSK Demodulated Waveforms
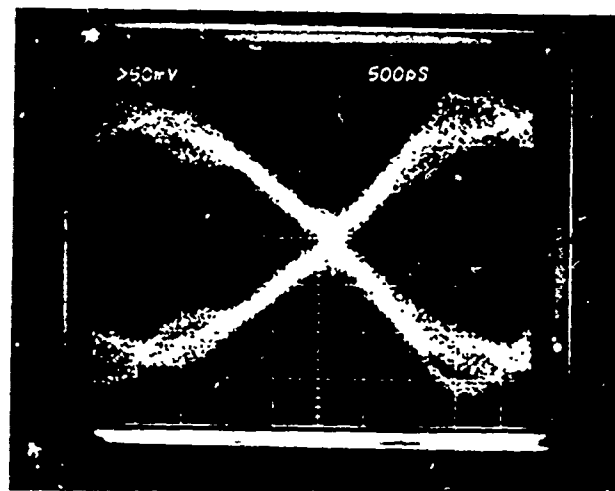
b) MSK Demodulated Signal Eye Pattern

Figure 23. Signals After Transmission Through the
Ka-Band Demonstration Link

19

2.3.2 Demonstration Link Tests/Coherent QPSK Modulation

The digital terminal and demonstration link were configured as shown in Figure 24 to characterize the performance of a system using coherent QPSK modulation. The results of these tests are summarized in Table 7. Testing included measuring the BER and photographing the modulated and demodulated waveforms.

TABLE 7. QPSK Ka-BAND DEMONSTRATION LINK
PERFORMANCE SUMMARY

Parameter	Performance
BER degradation at 1×10^{-6}	1.7 dB
Data transition time	1.9 nsec
Data asymmetry	±500 psec
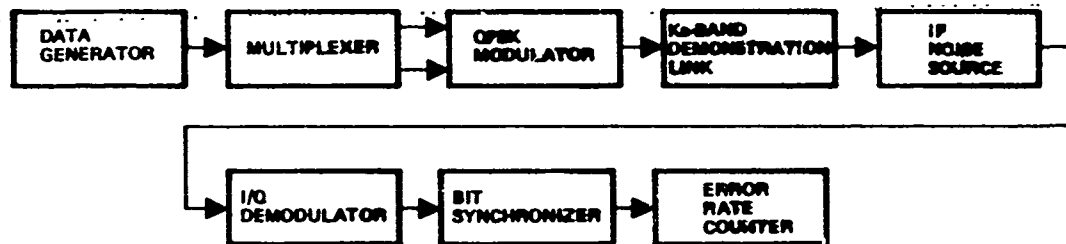
Figure 24. Coherent QPSK Demonstration Link Test Configuration

BER Tests

The BER performance of the Ka-band link using coherent QPSK modulation was measured over an E_b/N_o range of 9 to 14 dB. This was sufficient to vary the resulting bit error rate from $>10^{-4}$ to $<10^{-7}$. The measured degradation from theoretical was 1.7 dB at an error rate of 10^{-6} and increased slightly to 1.9 dB at 5×10^{-8}. The complete BER curve is shown in Figure 25. The incremental BER degradation of the system due to the Ka-band link was 0.7 dB. As was expected, this result is higher than the 0.2 dB measured for MSK and reflects the level of improvement available in link performance by using MSK over QPSK.

The BER testing of the link was repeated with the ADA bypassed to determine its effect on the link BER performance. With the ADA bypassed, the BER degradation was 1.7 dB compared to 1.9 dB with the ADA in the link. This result is just the reverse of what was found for MSK and is indicative of the lower tolerance of QPSK to link distortion.

20
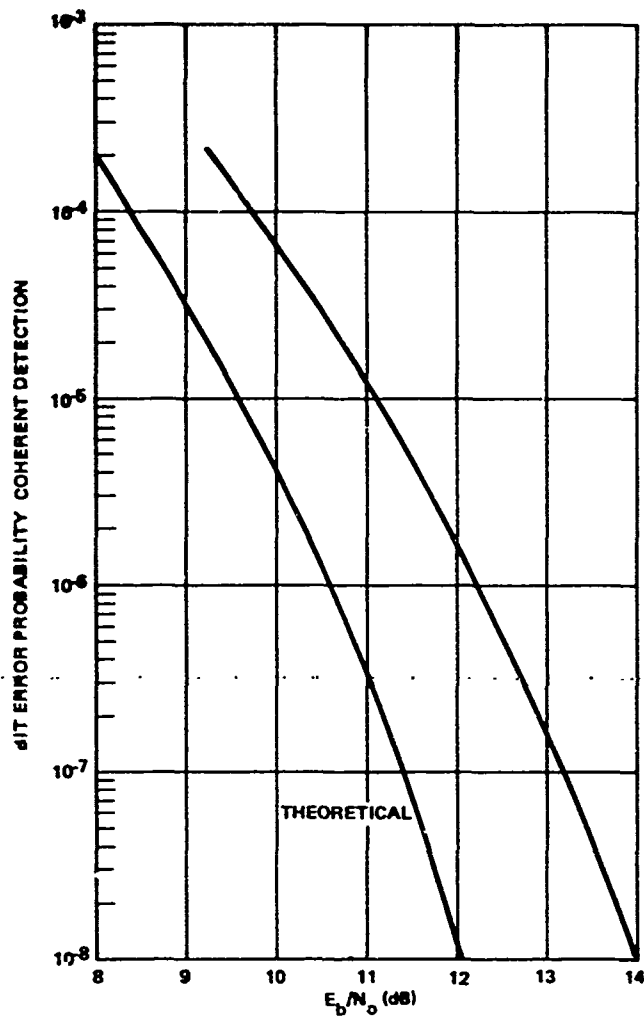
Figure 25.   Ka-Band Demonstration Link Coherent QPSK BER Performance

Spectrum Occupancy

The photograph of the spectrum occupancy of the coherent QPSK modulated signal after being transmitted through the complete Ka-band demonstration link is shown in Figure 26.   Compared to the coherent QPSK spectrum recorded directly at the output of the modulator (refer to Figure 14), there is little visible distortion to the modulated spectrum, other than a slight distortion in the tops of the energy lobes which fall on the skirts of the bandpass filter.   The effect of the limited link bandwidth is apparent from the photo.   After being transmitted through the link, the modulated energy levels at f_o ±450 MHz have been reduced from the unfiltered level of 20 dB below the peak level to >40 dB down.

Demodulated Waveforms

The waveforms at the output of the demodulator were recorded and analyzed to determine the demodulated transition time, data asymmetry. and overall quality of the

21
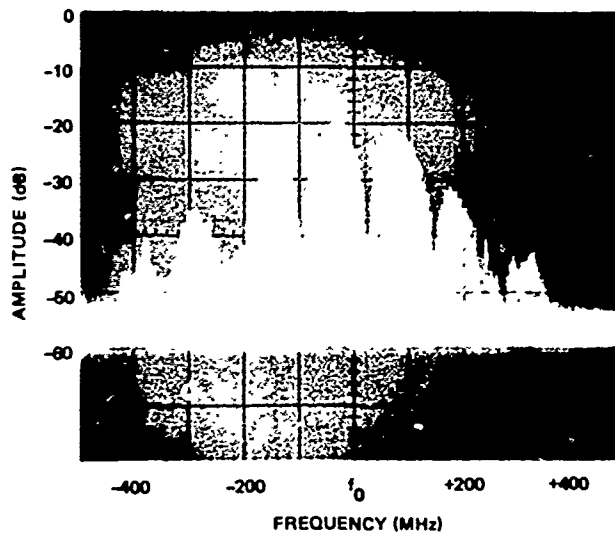
Figure 26. Coherent QPSK Modulator Spectrum after Transmission
Through the Ka-Band Demonstration Link

signal. These photographs are shown in Figure 27. The overview photograph shows 25 consecutive bits of the I and Q channels. The photo shows the increase in data transition time due to the link bandlimiting and the elimination of overshoot following transition due to saturation in the ADA.

The second photograph shows the demodulated transition times for the signal. The typical 10 to 90% transition time was 1.9 nsec, which is signficantly degraded from the 700 psec value measured directly at the output of the modulator. The final photograph is the eye pattern for the demodulated signal. Based on this photo, the worst case asymmetry is ±500 psec, compared to ±250 psec measured directly at the modulator output. The asymmetry degradation is due to the link nonlinearities which distort the shape of the bits, as a function of the data sequence. That is, a field of successive 1, 0, 1, 0 transitions will have higher asymmetry than a field of successive 1's or 0's. This effect can be seen in the overview photograph.

2.3.3 Demonstration Link Tests/Differentially Coherent QPSK Modulation

The digital terminal and demonstration link were configured as shown in Figure 28 to characterize the performance of the system using differentially coherent QPSK modulation. The results of these tests are summarized in Table 8. Testing included measuring the BER and photographing the modulated and demodulated waveforms.

TABLE 8. DIFFERENTIALLY COHERENT QPSK Ka-BAND DEMON-
STRATION LINK PERFORMANCE SUMMARY

Parameter	Performance
BER degradation at 1×10^{-6}	3.9 dB
Data transition time	1.2 nsec
Data asymmetry	±600 psec

22
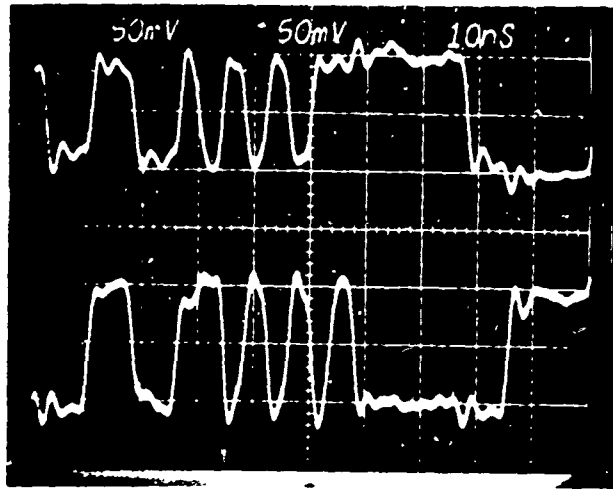
a) QPSK Demodulated Waveform
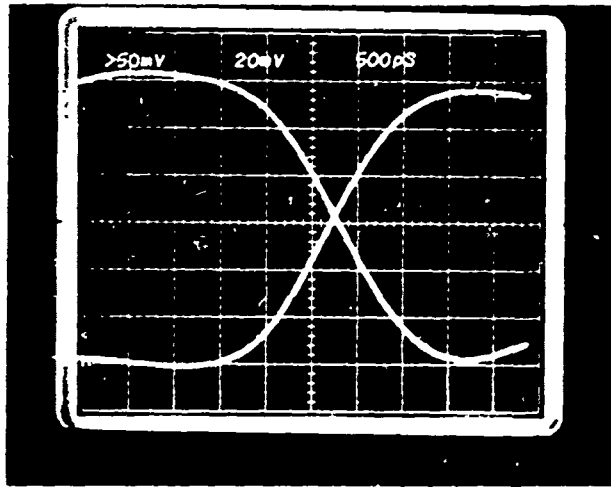
b) QPSK Demodulated Signal Rise and Fall Times
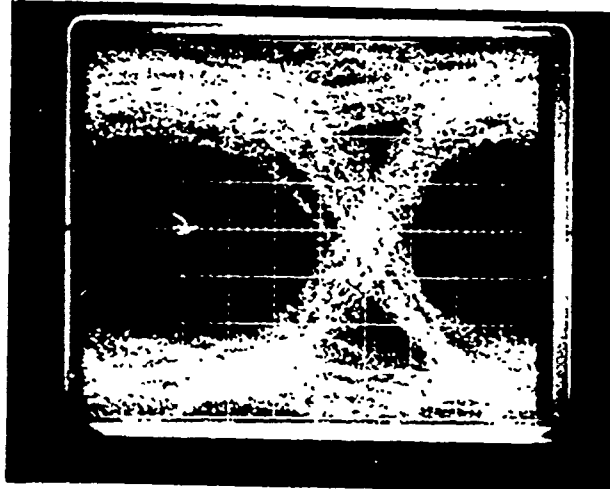
500 psec/division

c) QPSK Demodulated Eye Pattern

Figure 27. Signals After Transmission Through the
Ka-Band Demonstration Link

23
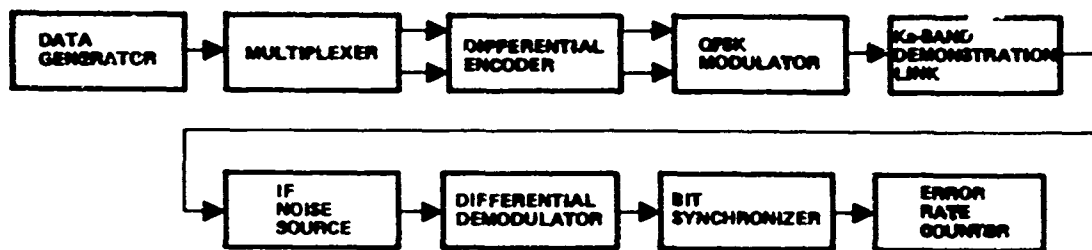
Figure 28. Differentially Coherent QPSK Demonstration Link Test Configuration

BER Tests

The BER performance of the Ka-band link using differentially coherent QPSK modulation was measured over an E_b/N_0 range of 13 to 19 dB. This was sufficient to vary the resulting error rate from $>10^{-4}$ to $<10^{-7}$. The measured degradation from theoretical was 3.9 dB at an error rate of 10^{-6}. The complete BER curve is shown in Figure 29.

The incremental BER degradation of the system due to the Ka-band demonstration link was 0.7 dB. This is the same result as was achieved for coherent QPSK and indicates that both forms of QPSK are equally degraded by the link distortions. It should be pointed out though that differentially coherent QPSK operates at an overall higher
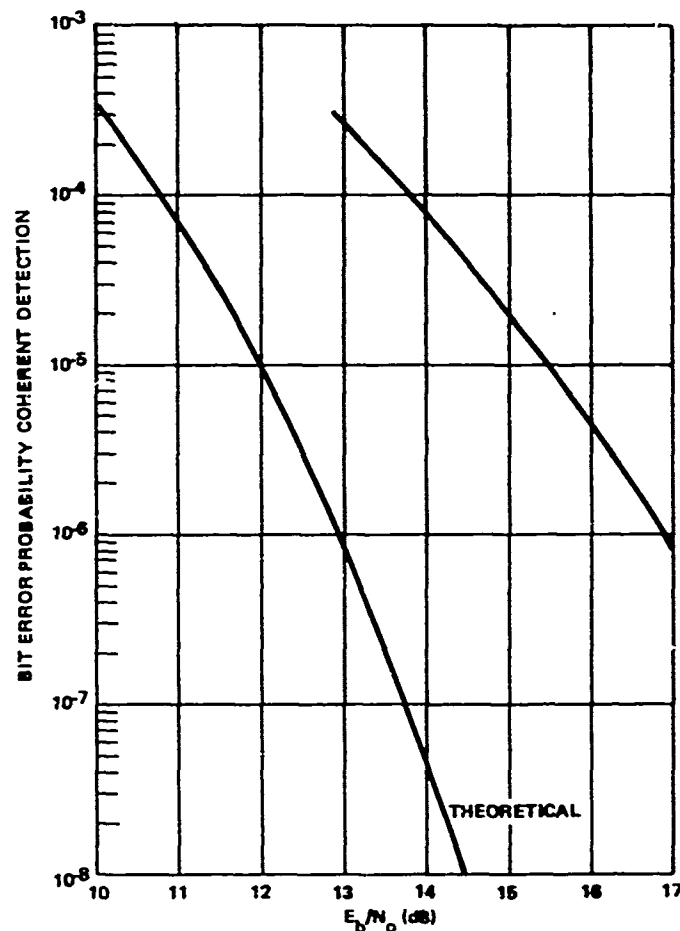
Figure 29. Ka-Band Demonstration Link Differentially Coherent QPSK BER Performance

24

error rate compared to coherent QPSK. Differentially coherent QPSK requires an E_b/N_o of 16.9 dB to achieve an error rate of 10^{-6} whereas coherent QPSK requires only 12.4 dB.

The BER testing of the link was repeated with the ADA bypassed to determine its effect on the link performance. With the ADA bypassed, the BER degradation increased to 4.6 dB, compared to 3.9 dB with the ADA. The BER improvement by the ADA is primarily due to saturation in that device.

The differentially encoded QPSK signal has significant AM on the waveform (100% at transition). This AM introduces significant distortion in the demodulated data due to the fact that the demodulator is both a phase and amplitude detector. Although the ADA does introduce passband distortion in addition to limiting the signal, the net result is to improve the link performance by 0.7 dB.

Spectrum Occupancy

The spectrum occupancy of the differentially coherent QPSK modulated signal after being transmitted through the complete Ka-band demonstration link is shown in Figure 30. All modulated energy outside of the ±300 MHz link bandwidth is >25 dB down compared to only 15 dB as measured directly at the modulator output. As previously explained in Section 2.2.3, the lines in the spectrum do not follow a sin x/x distribution because the differential encoding results in a data sequence which is no longer a maximal length PRN code.
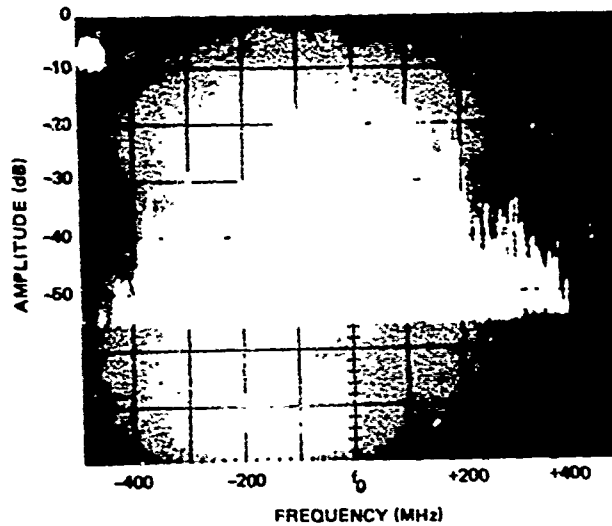
Figure 2-30. Differentially Coherent QPSK Modulated
Spectrum After Transmission Through
the Ka-Band Demonstration Link

Demodulated Waveforms

The waveforms at the output of the demodulator were recorded and analyzed to determine the demodulated transition time, data asymmetry, and overall quality of the signal. These photographs are shown in Figure 31. The overview photograph shows 25 consecutive bits of the I and Q channels.

When compared to the same photograph for coherent QPSK (Figure 27), the higher overall degradation in the demodulated signal is quite apparent. The second photograph shows the demodulated transition times for the signal. The typical 10 to 90% transition time was 1.2 nsec, which is significantly degraded from the 300 psec value measured directly at the modulator output. The final photograph is the eye pattern for the demodulated signal. Based on the photo, the worst case asymmetry throughout the code is ±600 psec, compared to ±350 psec measured directly at the modulator output. The ±600 psec asymmetry value is extremely high and in part explains the poor performance of differential QPSK.

26
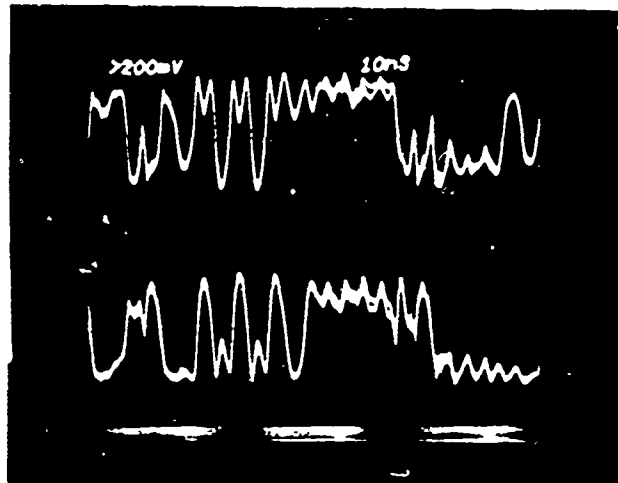
a) Differentially Coherent QPSK Demodulated Waveforms
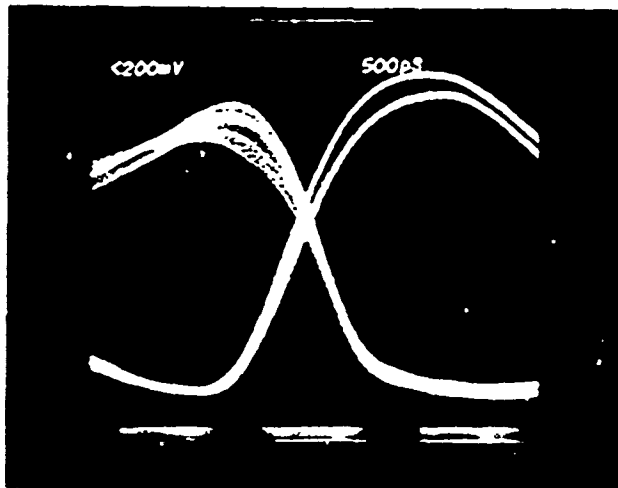
b) Differentially Coherent QPSK Rise and Fall Times
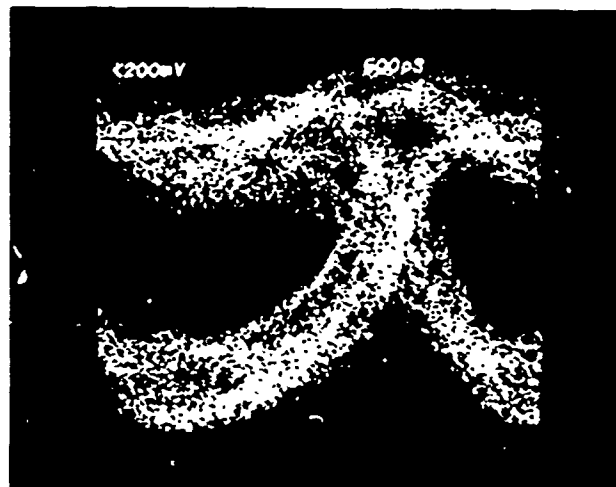
c) Differentially Coherent QPSK Eye Pattern

Figure 31. Differentially Coherent QPSK After Transmission
Through the Demonstration Link

27

SECTION III
HARDWARE DESCRIPTION

Two sets of equipment were assembled to perform this test program: a Ka-band demonstration link and a digital terminal. Both of these items were configured using commercial test equipment and special circuits and components designed by TRW. This section describes these components in detail.

3.1 KA-BAND DEMONSTRATION LINK DESCRIPTION

The Ka-band demonstration link includes all of the equipment (with the exception of antennas) necessary to completely simulate an actual data link. The link accepts a wideband (600 MHz) S-band input and translates it to Ka-band (38 GHz). The signal is then amplified to an output level of 100 mW. After attenuation to simulate path loss, the signal is downconverted back to S-band, where it is then demodulated in the digital terminal. The demonstration link consists of five major subassemblies:

- S-band frequency sources

- X9 multiplier/avalanche diode oscillator

- Doubler/upconverter

- Avalanche diode amplifier

- Downconverter.

Each of these components is discussed in detail in the following sections. The complete demonstration link is shown in Figure 32.
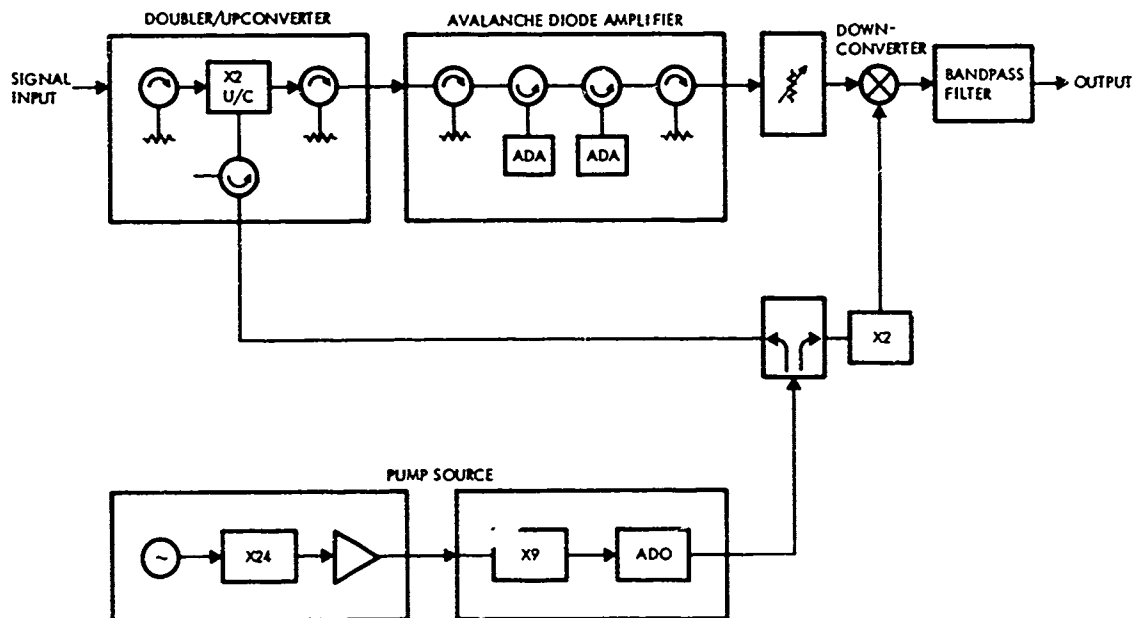
Figure 32. Ka-Band Demonstration Link

28

3.1.1 S-Band Frequency Sources

Two S-band frequency sources are used in the demonstration link. The first (2.144 GHz) serves as the carrier source to the modulator. The second serves as the input to the S to Ka-band frequency multiplier chain. The sources utilize space-qualified electrical and mechanical design concepts which incorporate mechanically standardized alumina microstrip modules. A photograph of one of the sources is shown in Figure 33.
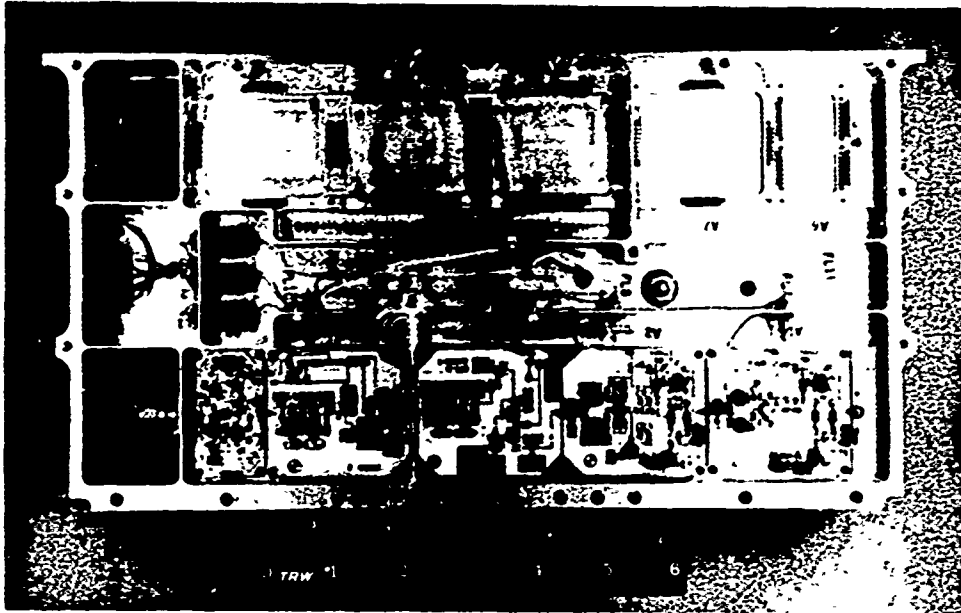
Figure 33. S-Band Frequency Source

Conceptually, the S-band sources consist of a stable crystal oscillator followed by low order frequency multipliers, interstage amplifiers, and filters. A total multiplication factor of 24 is achieved using three successive multiplier stages: X2, X2, and X6. The pump source has a final output frequency of 2.063 GHz and provides an output level of ±25 dBm. Table 9 summarizes its performance. The carrier source is similar to the pump source. The only difference is that the final output frequency is 2.144 GHz and the output power level is +10 dBm.

3.1.2 X9 Multiplier

The X9 multiplier consists of a single-step high order varactor diode multiplier followed by an injection-locked avalanche diode oscillator (ADO). An output power level of +23 dBm is achieved at 18.077 GHz. A photograph of the multiplier is shown in Figure 34.

The X9 multiplier consists of an S-band input matching network mounted in a rectangular cavity located on top of the waveguide mount containing the varactor diode. The output from the diode, which is mounted in reduced height waveguide, is passed through an impedance transformer into a separate waveguide output filter. Idler tuning

29

TABLE 9.— PERFORMANCE SUMMARY OF THE S-BAND
FREQUENCY SOURCE

Parameter	Performance
Output frequency	2.06333 GHz
Output power	+25 dBm
DC power	200 mA at 15 V* 3.0 watts
DC to RF efficiency	10.5%
Spurious output	22 dBc for 2nd harmonic 50 dBc for 4th harmonic >70 dBc for all other frequencies

*Includes an integrated voltage regulator.
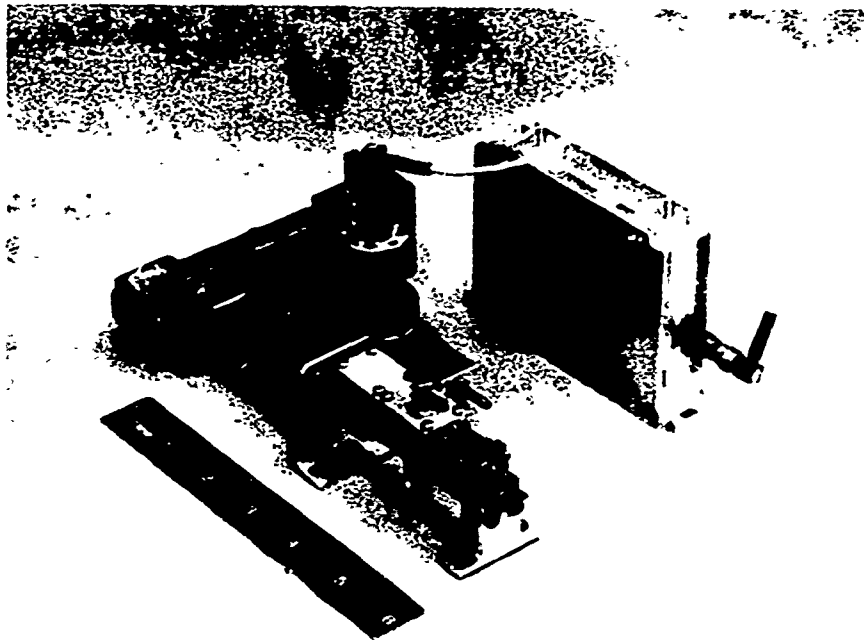
Figure 34. X9 Multiplier/Avalanche Diode Oscillator

is obtained by the introduction of waveguide shims between the flanges connecting the diode mount and the output filter. A coaxial lowpass filter is used to couple the input signal to the multiplier diode.

The X9 multiplier drives an injection-locked avalanche diode oscillator. The oscillator circuit utilizes a 0.020" high, reduced height waveguide, with double step transformers to full height output waveguides. A triple screw tuner with $\lambda_g/4$ screw spacings is located in the full height guide for RF tuning. Fabrication of the wave-guide diode mount was similar to the multiplier diode mount. The bias circuit was con-

structed as a length of coaxial air line bolted to the body of the waveguide. A five-port waveguide circulator is used to couple the multiplier to the injection-locked oscillator and to provide isolation between the multiplier/oscillator and oscillator output interfaces. The injection-locked ADO has an output power of +23 dBm at 18.077 GHz.

3.1.3 Doubler/Upconverter

The doubler/upconverter combines the functions of a frequency doubler and an upconverter into a single circuit. The pump frequency (18.077 GHz) is doubled and combined with the signal (2.144 GHz) using a parametric varactor diode circuit. The resulting output frequency is $f_o = 2f_{pump} \pm f_{signal}$. The correct output frequency is selected by a multisection waveguide filter on the output port. The pump input port also has a filter which prevents the upconverted output signal from propagating out the pump port. The module, as shown in Figure 35, is constructed with an electroformed cruciform structure in which the input and output waveguides are perpendicular to each other. This type of construction allows each port to be optimized with a minimum of interaction with the other port. The modulated carrier is injected into the GaAs varactor diode via a combination lowpass filter and matching section mounted at the intersection of the two waveguides and is perpendicular to the plane of the waveguides. The combined doubler/upconverter results in fewer component parts and a more efficient system because a doubler/upconverter has less conversion loss than a doubler followed by an upconverter.
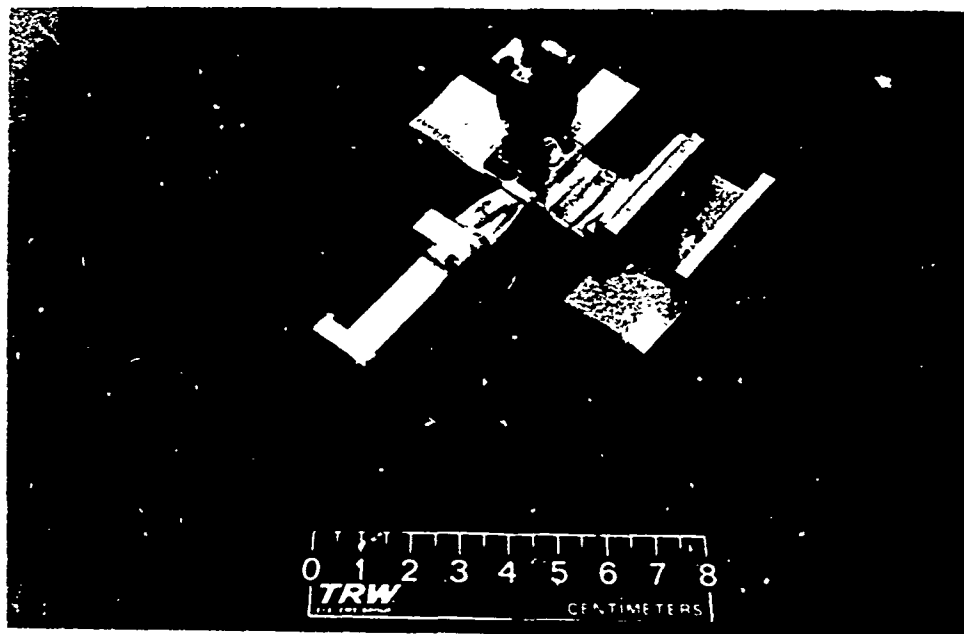
Figure 35. Doubler/Upconverter

31

3.1.4 Avalanche Diode Amplifier

The output amplifier in the link (Figure 36) is a two-stage circuit using avalanche diodes in a negative resistance mode. The negative resistance amplifier is a one-port device in which the input and output signals coexist within one transmission line. In order to obtain a useful amplifier, separate input and output ports are created using a waveguide circulator. The circulator directs the input signal into the amplifier and couples the amplified output signal to the output port.
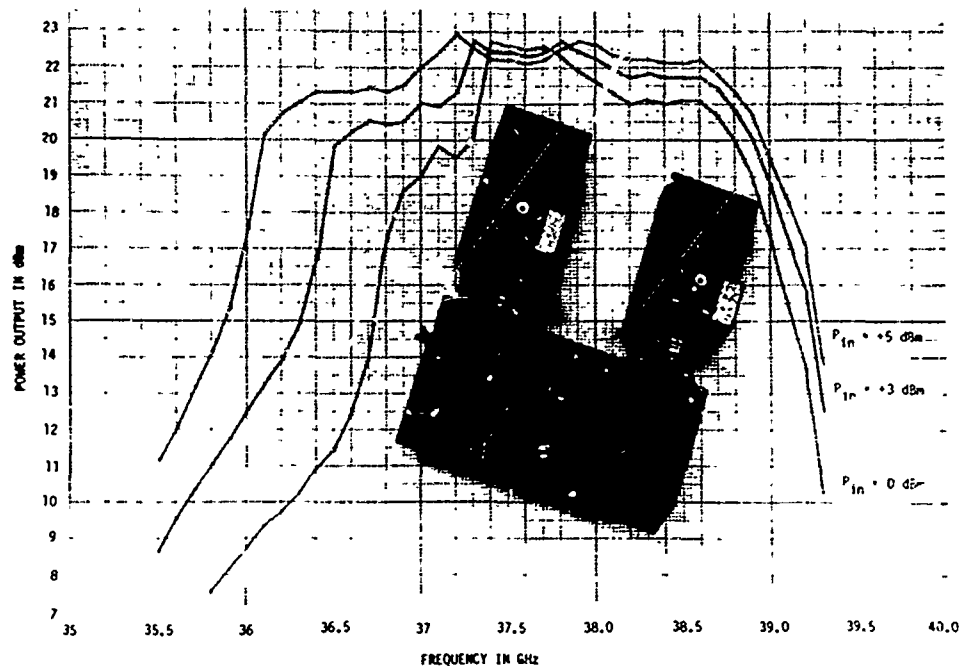
Figure 36. Avalanche Diode Amplifier

The ADA consists of two separate amplifier modules series-coupled by a five-port (three-junction) circulator. The modules utilize silicon Impatt diodes mounted in a 0.20" reduced height waveguide. The mounts, which must function as high quality neat sinks, are machined out of tellurium copper in a split block configuration. Electroformed quarterwave step transformers couple the mount to the circulator. Completing the assembly are dc current regulators, one for each diode.

The individual stages within the Ka-band ADA exhibit characteristics found in lower frequency multistage power amplifiers. The first stage amplifies the low input level (0 dBm) with high gain (12 dB). The output level (+20 dBm) is provided by the second stage but with reduced gain (8 dB). The ADA operates in saturation (5:1 signal compression) and requires 10 watts of dc power (145 mA at 26 volts and 230 mA at 27 volts), excluding power dissipated in the current regulators.

3.1.5 Ka-Band Downconverter

The final assembly in the demonstration link is the Ka-band downconverter. It consists of a Ku to Ka-band doubler, a balanced mixer downconverter, and an S-band bandpass filter.

32

The construction of the doubler is very similar to the doubler/upconverter. The Ka-band doubler is a cruciform waveguide structure with the input and output waveguides perpendicular to each other. The GaAs varactor diode is mounted at the intersection of the waveguides. The diode is self-biased using an external resistor network which is RF decoupled from the varactor with a lowpass filter. The input and output ports of the doubler have tuning screw matching networks and bandpass filters.

The downconverter mixer is a standard commercial component. The mixer (Spacekcom PN C37-2.4) downconverts the 38.299 GHz input signal to 2.144 GHz using the 36.155 GHz local oscillator output from the doubler. The final component in the downconverter is a bandpass filter. The filter is a commercial tubular design and sets the overall link bandwidth.

3.2 DIGITAL TERMINAL DESCRIPTION

The digital terminal (Figure 37) served as both the source of the input signal to the demonstration link and as the data receiver. Although the test set was configured to operate at 250 Mbps per channel, it is capable of performing BER measurements at data rates of up to 600 Mbps per channel (1.2 Gbps QPSK or MSK) and consists of the following equipment:

- Tau-Tron PRN code data generator
- Multiplexer
- Differential encoder
- QPSK and MSK modulators
- IF noise source
- I-Q demodulator
- Differential demodulator
- Bit synchronizer
- Demultiplexer
- Tau-Tron error rate counter.

3.2.1 Multiplexer

The multiplexer accepts the single $2^7 - 1$ PRN code from the Tau-Tron generator and creates separate I and Q channels. In addition, the multiplexer is used to double the 100 to 300 Mbps data rate of the generator when required. The multiplexer generates two channels by dividing the input data stream. One-half is amplified and becomes the I channel. The other half is inverted and delayed by 2 bits and serves as the Q channel. Finally, both data streams are reclocked to ensure low data asymmetry.

33
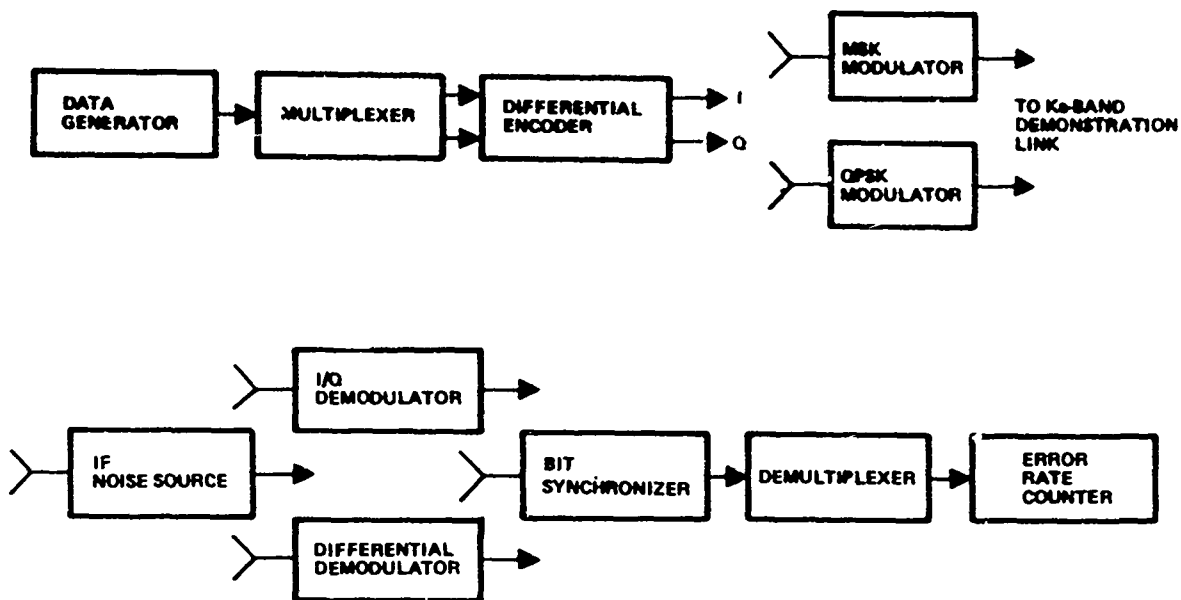
Figure 37. Digital Terminal

3.2.2 <u>Differential Encoder</u>

Differentially coherent QPSK is a modification of coherent QPSK, where each symbol is represented as a phase change between successive bits rather than an absolute phase state. The differential encoding technique allows the quadriphase data system to operate without generating a coherent phase reference in the system demodulator. Basically, the differential encoded system uses the state of the previous data bit as a comparison reference in decoding the current data bit. The differential encoder adds the current data bit to the previous data bit and encodes the sum of the two — for example, previous state $1(0,1)$, current state = $2(1,0)$, and encoded output = $2(1,1)$. The data is decoded by the reverse process. The received data = $3(1,1)$, previous data = $1(0,1)$, and data output = $2(1,0)$. Table 10 summarizes the operation of the differential encoder. Input data bit pairs are compared to the last state data pair inputs and the corresponding data outputs appear in the resulting matrix.

TABLE 10. DIFFERENTIAL ENCODER AS A FUNCTION OF INPUT WORD

Input Symbol (a_n, b_n)	Previous Input Symbol (a_{n-1}, b_{n-1})			
	1,1	0,1	0,0	1,0
1,1	1,1	0,1	0,0	1,0
0,1	0,1	0,0	1,0	1,0
0,0	0,0	1,0	1,1	0,1
1,0	1,0	1,1	0,1	0,0

34

The differential encoder has been implemented with the logic flow diagram shown in Figure 38. Basically the logic state of the previous output is fed back to the input NOR gates. This results in the desired phase change referenced data coding.
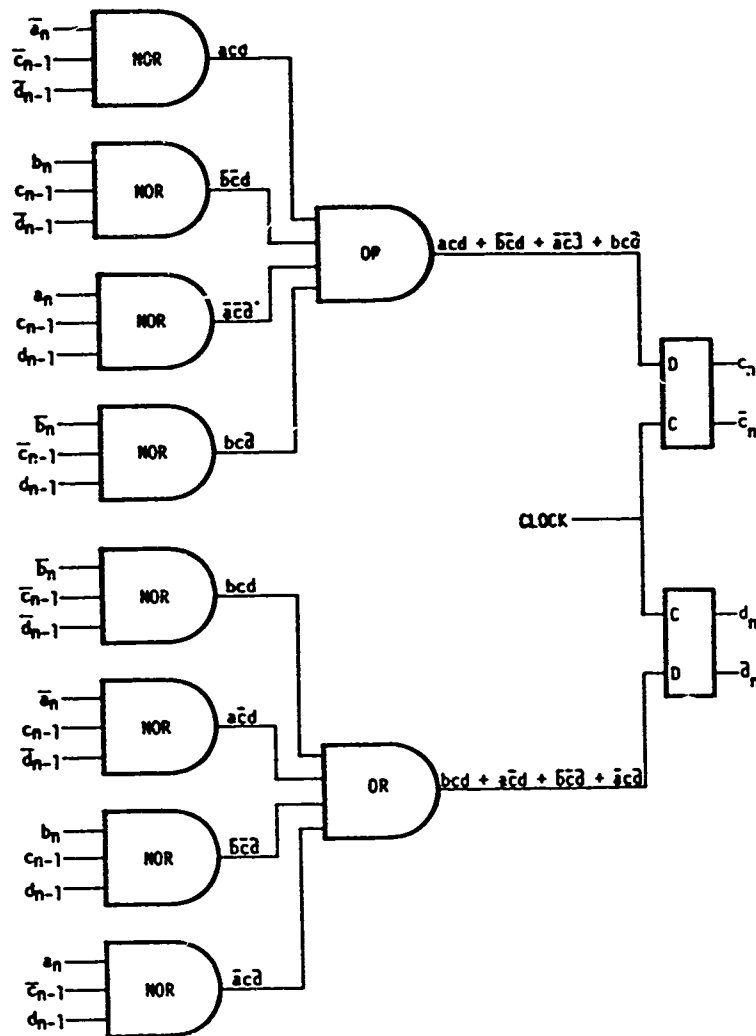
Figure 38. Differential Encoder Implementation

3.2.3 QPSK Modulator

The QPSK modulator is a standard parallel configuration as shown in Figure 39. The 2.144 GHz carrier is split into two equal amplitude quadrature channels by a 90° hybrid. Each of the two channels is then biphase (0° and 180°) modulated by the input data. The output of the two modulators is in-phase power combined to generate the quadriphase modulated output signal. All of the modulator components are standard commercial items with the exception of the data amplifiers. The data amplifiers are a TRW design which utilizes microwave transistors in order to obtain switching speeds

35

compatible with high data rate transmission. The biphase modulators are standard commercial doubly-balanced mixers. Phase and amplitude adjustments are accomplished by means of compensation circuits which have adjustable phase and amplitude characteristics. The complete QPSK modulator is assembled in a machined aluminum housing using SMA connectors and flex cable fo: RF component interconnects.
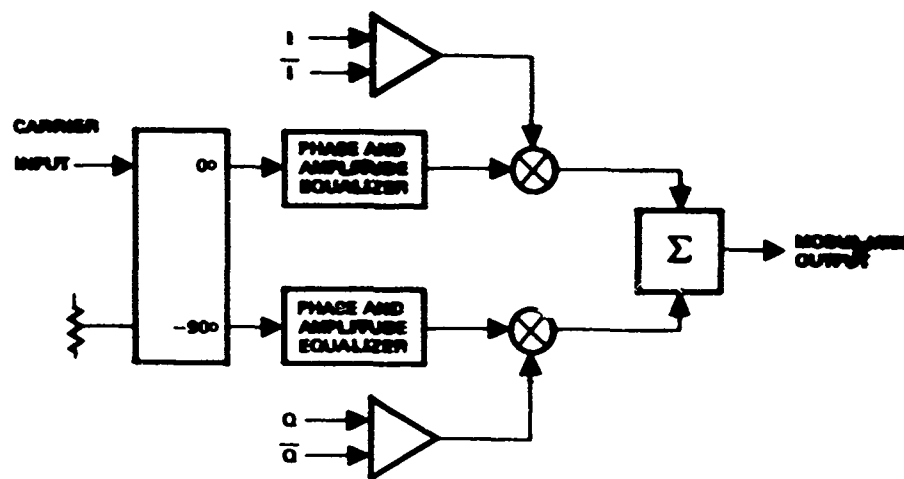
Figure 39.   QPSK Modulator

3.2.4 MSK Modulator Description

The design of the MSK modulator is based on the quadrature pulse amplitude modulation properties of MSK. The basis for the modulator design is best understood by examining the expression for the MSK waveform. The waveform can be expressed as

$$M(t) = a(t) \cos t \frac{\pi t}{T} \cos \omega_0 t + b(t) \sin \frac{\pi t}{T} \sin \omega_0 t \qquad (1)$$

where $a(t)$ and $b(t)$ are the modulating data sequences skewed by one-half symbol, and T is the symbol time.

It is clear that the waveform contains two carrier terms: $\cos \omega_0 t$ and $\sin \omega_0 t$ which are amplitude modulated by two terms $a_k \cos \pi t/T$ and $a_{k+1} \sin \pi t/T$. By squarewave modulating these two terms by Σa_k and $-\Sigma a_{k+1}$, respectively, and summing the two terms, the result is an MSK modulated waveform.

The circuit shown in Figure 40 is an MSK modulator of the type just described. The two modulated carriers are generated by mixing the carrier $\cos \omega_0 t$ with the clock $\cos \pi t/T$. The two tones resulting from this mixing process are

$$f_a = \frac{1}{2} \cos (\omega_0 t + \frac{\pi t}{T}) \qquad (2)$$

$$f_b = \frac{1}{2} \cos (\omega_0 t - \frac{\pi t}{T}) \qquad (3)$$
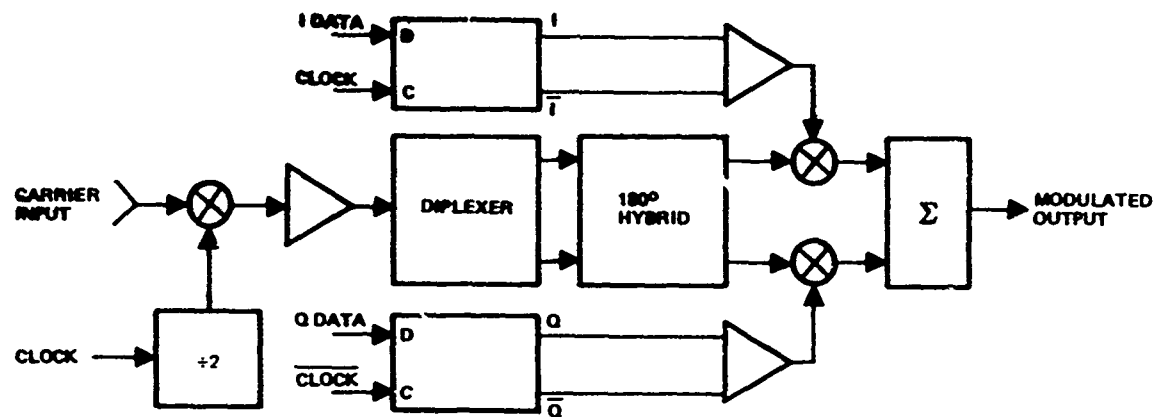
Figure 40. MSK Modulator

These two frequency tones are then separated by a diplexer and applied to the inputs of
a magic tee hybrid. The two output signals from the hybrid are

$$f_c = \frac{1}{2}(f_a + f_b) \tag{4}$$

$$= \cos \omega_0 t \cos \frac{\pi t}{T} \tag{5}$$

$$f_d = \frac{1}{2}(f_a - f_b) \tag{6}$$

$$= \sin \omega_0 t \sin \frac{\pi t}{T} \tag{7}$$

Finally, these two signals are multiplied by +1 or -1 by biphase modulators and summed.
The phases of f_c and f_d are adjusted so that the biphase switch transitions when the
instantaneous amplitude of these signals is zero. The four possible output stages of
the modulator can then be expressed as

$$f_e = \pm \cos \omega_0 t \cos \frac{\pi t}{T} \pm \sin \omega_0 t \sin \frac{\pi t}{T}$$

$$= \pm \cos \left(\omega_0 \pm \frac{\pi}{T} \right) t$$

Provision is made to adjust the phase and amplitude of the signals in the modulator to
optimize the balance of the four output stages. The amplitude is adjusted with variable
attenuators and the phase is trimmed with circulator coupled sliding shorts. All of the
components used in the modulator are standard commercial components which have been
specifically selected and optimized to meet the performance requirements of the modula-
tor. The same biphase switches and modulator driver amplifiers that are used in the
S-band QPSK modulator are used in the MSK modulator. These switches are capable of
biphase switching rates of >400 Mbps and transition times of <500 psec. The remaining

components in the modulator have all been chosen to maximize the performance of the modulator. The magic tee hybrid and the in-phase power combiner have been carefully selected for minimum phase and amplitude imbalance in their respective power splits.

3.2.5 IF Noise Source

Broadband noise is reactively summed with the modulated carrier prior to demodulation to create an effective E_b/N_o at the demodulator input. The noise source shown in Figure 41 generates noise by amplifying thermal noise by 64 dB and bandlimiting it to 600 MHz. The E_b/N_o was determined from the received modulated signal power, noise power spectral density, and detection filter bandwidth.
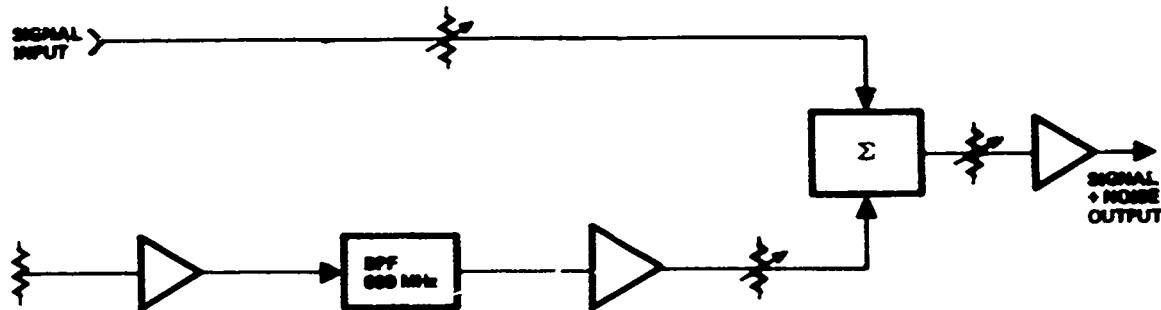
Figure 41. IF Noise Source

3.2.6 Quadriphase Demodulator

The demodulator extracts the data from the received signal by multiplying the incoming modulated signal by the recovered carrier. The demodulator is a standard data demodulator using a carrier recovery loop with decision feedback (also known as a modulation-wipeoff carrier recovery loop). The demodulator, shown in Figure 42, consists of three basic circuits: a quadrature demodulator, a QPSK remodulator, and a phase-locked carrier recovery loop. The modulated input signal is first split into I and Q components by an in-phase power divider. The two signals are then phase-detected by a pair of double balanced mixers. The LO input to the mixers is the recovered carrier which has been power divided by a 90° hybrid. If the recovered carrier is coherent with the modulated carrier, then the IF outputs from the mixers represent the phase differences between the LO and the modulated carrier and are therefore the baseband data. The baseband data is next amplified and then power divided three ways to provide outputs to the bit synchronizer, the remodulator section, and front panel test points.

The demodulated baseband signals are used to remodulate the locally generated carrier. If the recovered carrier is coherent with the modulated carrier, then the original QPSK modulated signal and the remodulated QPSK signal will be identical in phase. The remodulated QPSK signal is fed to the phase detector and is the reference

38

Figure 42. I-Q Quadriphase Demodulator

with which a sample of the incoming signal is compared. A VCXO error signal is generated within the phase detector which corresponds to the phase difference between the modulated and remodulated signals. A delay line is necessary to delay the modulated signal for a period of time equal to the delay of the demodulation/remodulation process. In addition to the necessary loop filters and amplifiers, the phase-locked loop contains sweep circuitry for automatic signal acquisition.

3.2.7 Differential Demodulator

The differentially encoded data is demodulated by a relatively simple technique. The modulated input signal is split into two channels by an in-phase power divider. One channel is used to drive a quadrature data detector by means of a 90° hybrid and a pair of balanced mixers. The second channel is delayed by 1 bit and is used as the reference in the balanced mixer detectors. Therefore, the previous data bit is used as the phase reference to demodulate the current bit. The block diagram of the differential demodulator is shown in Figure 43.

3.2.8 Bit Synchronizer

The bit synchronizer performs two functions: clock recovery and bit decision, i.e., a best estimate of the digital data on a bit-by-bit basis. The bit synchronizer accepts the output data from the demodulator, which is a composite of signal and noise, determines the data state, and outputs this decision. A block diagram of the bit synchronizer is shown in Figure 44.

39
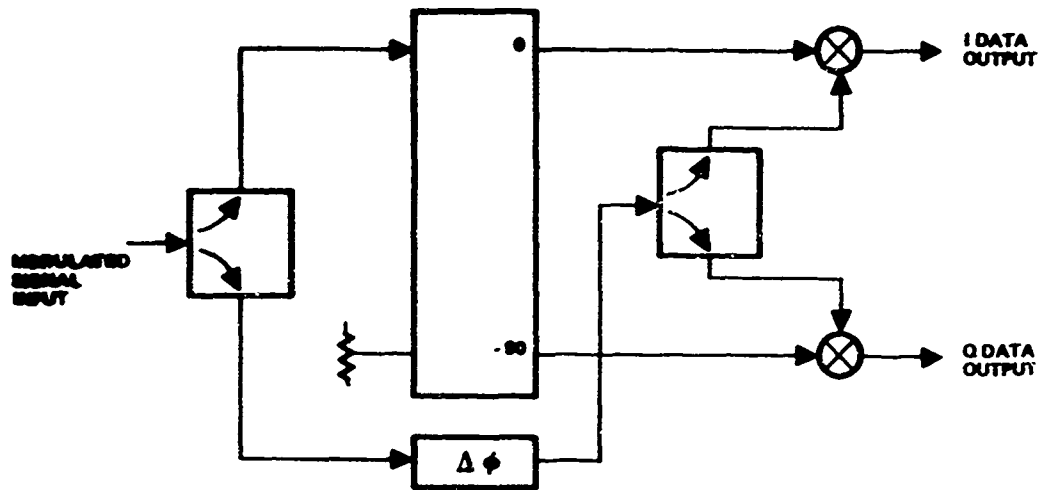
Figure 43. Differential Demodulator
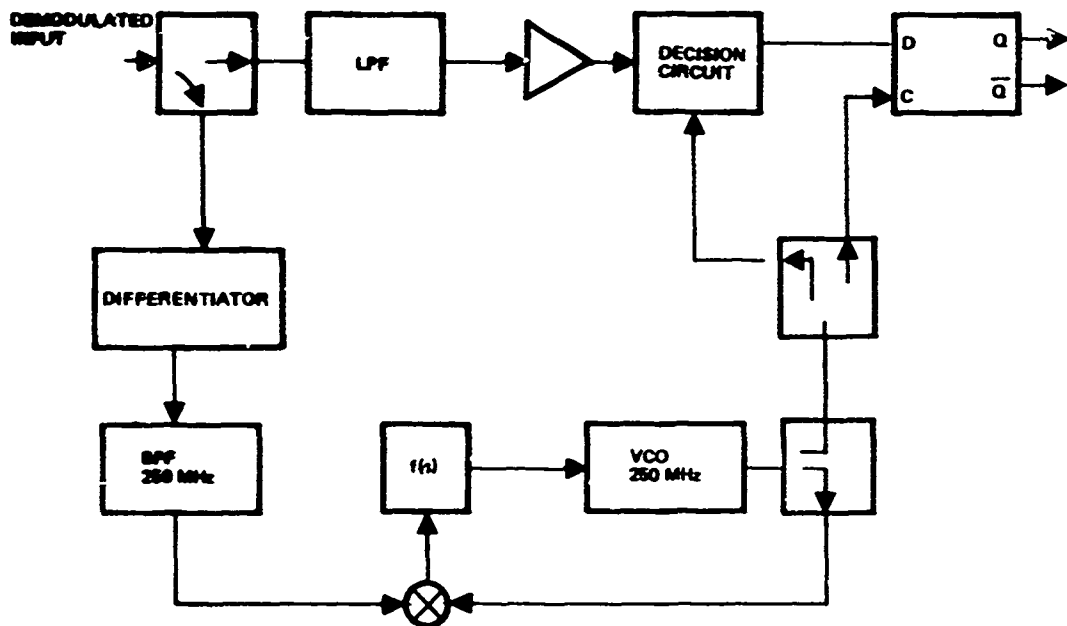
Figure 44. Bit Synchronizer

The data clock is recovered by differentiating the data. The output of the differentiator, which is a series of spikes at the clock frequency, is bandpass filtered to extract a sinusoid at the clock frequency. This signal is then used to phase-lock a VCXO which in turn provides a constant amplitude, stable frequency, low phase noise clock signal which is also used by subsequent digital circuits.

3.2.9 Demultiplexer

The demultiplexer is used only when the system is configured for MSK operation. The circuit consists of two type D flip-flops which are alternately clocked at one-half the data rate. Therefore each flip-flop is set by every other data input. The output of one of the flip-flops is inverted, which effectively inverts the state of every other input bit. If the two outputs are multiplexed, the original data would be regenerated. However, the Tau-Tron data detector can accept the data and delayed data outputs directly. The two data outputs are true PRN data sequences which are bit error rate counted by the Tau-Tron data detector. A block diagram of the demultiplexer is shown in Figure 45.
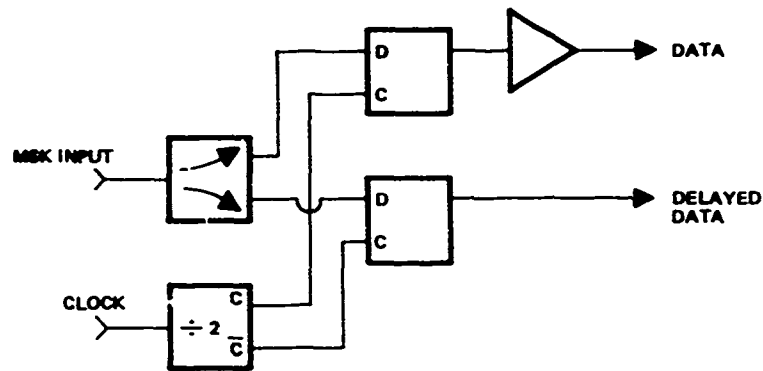
Figure 45. Demultiplexer

APPENDIX
WIDEBAND DIGITAL TRANSMITTER/RECEIVER TEST PLAN

The purpose of these tests is to evaluate the bit error rate performance of the digital Ka-band link at a data rate of 500 Mbps. The tests are to be conducted using QPSK and MSK modulation. In addition, the QPSK testing is conducted using both coherent and differentially coherent demodulation. The test program is organized into:

- Ka-band link passband characterization
- Digital terminal BER testing
- Link BER testing.

The test program is to be conducted over a 7 week period as shown in Figure A-1.

Figure A-1. Test Schedule

A block diagram of the equipment which has been assembled to perform the testing is shown in Figure A-2. The equipment is separated into two major functions: digital terminal and Ka-band wideband demonstration link. The digital terminal consists of a data generator, a differential encoder, S-band QPSK and MSK modulators, a noise source, coherent and differentially coherent demodulators, a bit synchronizer, and an error rate counter. The demonstration link consists of an S to Ka-band upconverter, an avalanche diode amplifier, a low noise downconverting mixer, and a bandlimiting filter.

The purpose of the testing program is to reliably and accurately compare the performance of the three modulation/demodulation techniques. The primary basis for the comparison is the relative bit error rate performance while the spectral occupancy or system bandwidth is being held constant. In addition to the BER tests, frequency and time domain measurements are performed to determine the spectral occupancy of the signal and the effects of bandlimiting on the transition time and asymmetry of the demodulated signal. The sequence of tests described in this test plan documents the relative performance of QPSK vs MSK and provides information necessary for configuring future high data rate digital links.

42
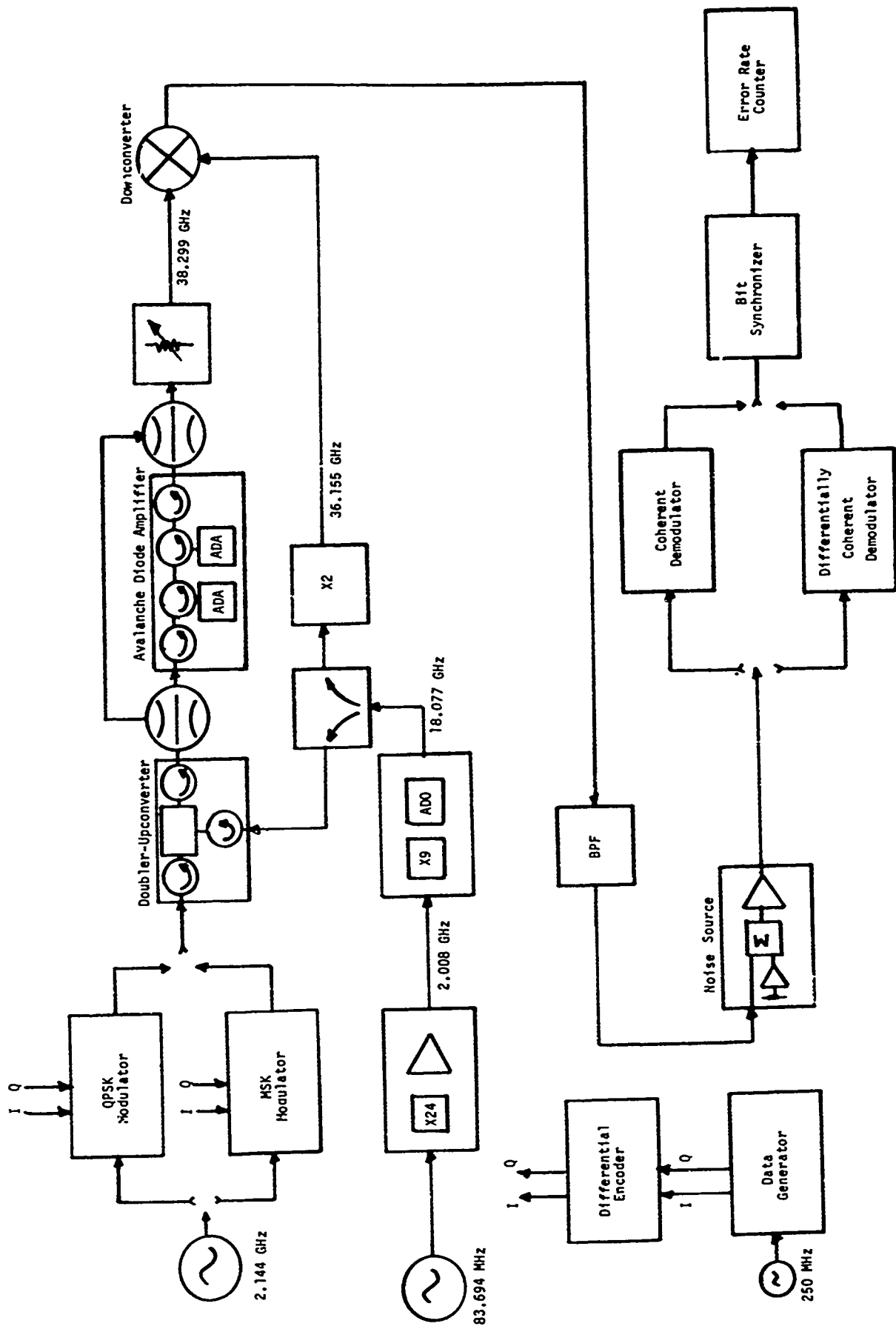
Figure A-2. Wideband Digital Transmitter/Receiver Equipment

1. LINK PASSBAND CHARACTERIZATION

Purpose: To characterize the microwave components used to assemble the Ka-band wideband demonstration link.

Procedure: The swept phase and gain of each component (Figure A-2) are measured using the test equipment shown in Figure A-3. The input power is varied above and below the nominal value for each component to determine the AM/AM and AM/PM conversion in each component. Table A-1 summarizes the tests performed, the data recorded, and the data analysis performed to characterize the Ka-band demonstration link. All of the measurements are taken over a 600 MHz bandwidth centered about a frequency of 2.144 GHz.

TABLE A-1. LINK PASSBAND MEASUREMENT SUMMARY

Equipment Under Test	Data Recorded		Measurement Range							Data Reduction						
	Swept Gain	Swept Phase	$P_N + 2$ dB	$P_N + 1$ dB	$P_{Nominal}$	$P_N - 1$ dB	$P_N - 2$ dB	$P_N - 4$ dB	$P_N - 6$ dB	1 dB Bandwidth	3 dB Bandwidth	10 dB Bandwidth	Phase Nonlinearity	Passband Ripple	AM/AM	AM/PM
U/C - D/C	X	X	X	X	X	X	X	X	X		X	X	X	X	X	X
U/C - ADA - D/C	X	X	X	X	X	X	X	X	X		X	X	X	X	X	X
BPF	X	X			X					X		X	X	X		
U/C - ADA - D/C - BPF	X	X	X		X		X					X	X	X		

U/C – UPCONVERTER   D/C – DOWNCONVERTER   ADA – AVALANCHE DIODE AMPLIFIER   BPF – BANDPASS FILTER
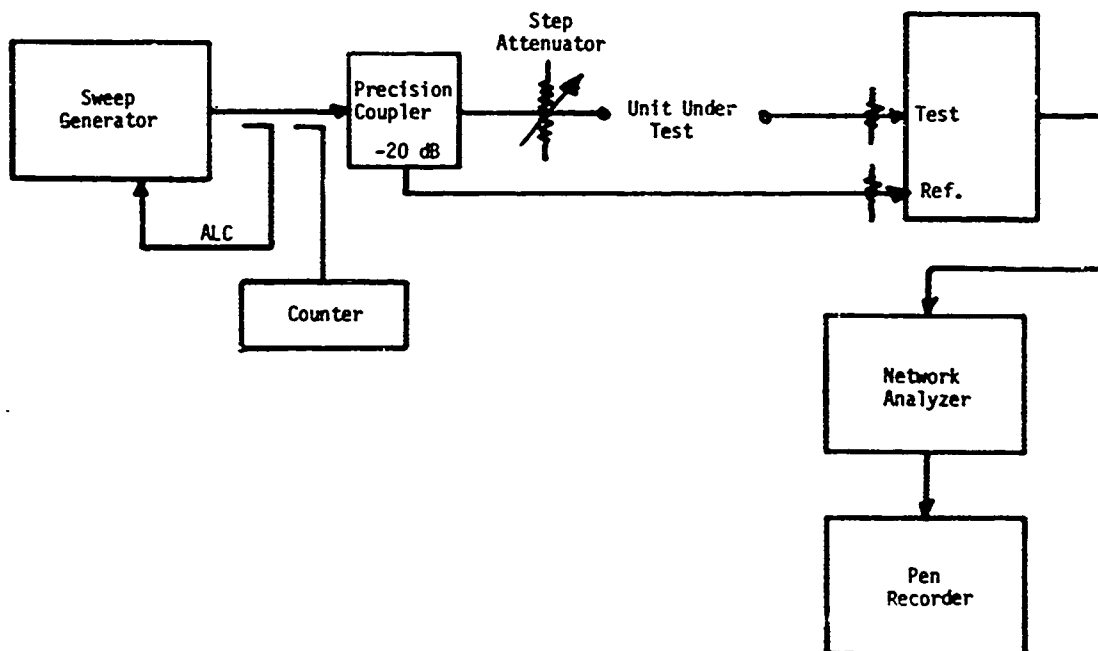
Figure A-3. Swept Measurement Test Equipment

44

2. DIGITAL TERMINAL TESTS

Purpose: To determine the bit error rate performance of the digital test equipment. The equipment to be tested includes the S-band QPSK and MSK modulators, the coherent and differentially coherent demodulators, and the bit synchronizer.

Procedure: The equipment under test is configured as shown in Figure A-4. The modulator/demodulator configurations to be evaluated are:

Modulator	Demodulator
QPSK	Coherent
QPSK	Differentially coherent
MSK	Coherent

The modulated (QPSK or MSK) S-band signal is directly demodulated. The only post modulation distortion introduced is due to the S-band amplifier following the modulator. The results of these tests indicate the BER performance of the digital terminal alone.
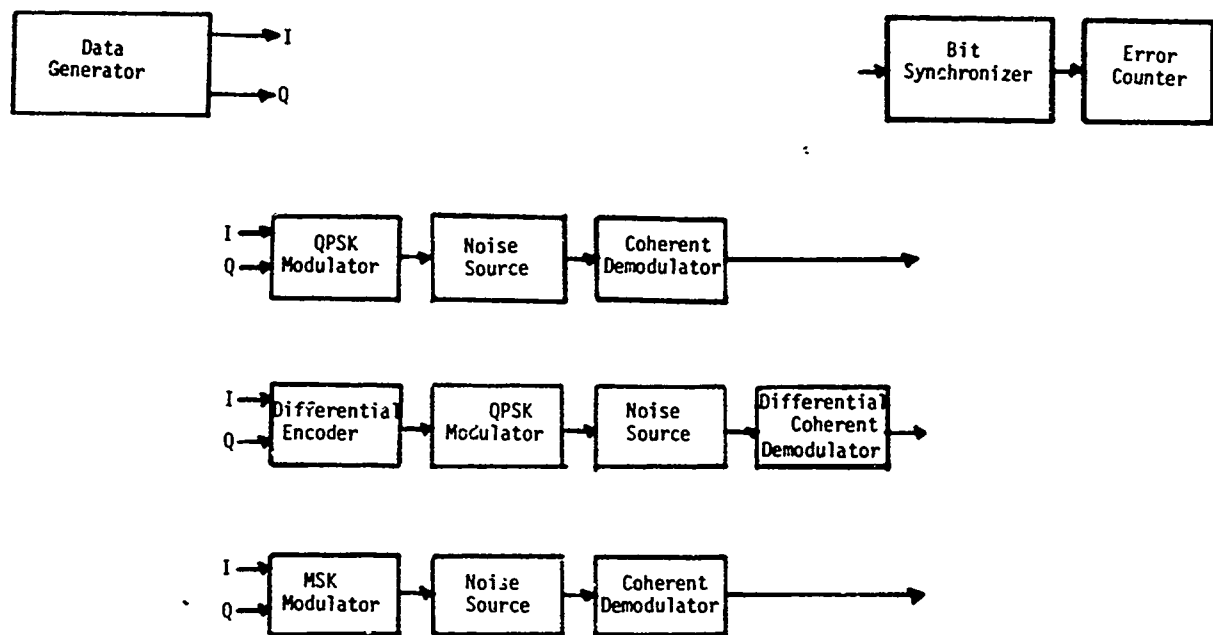
Figure A-4. Digital Terminal Test Configuration

The BER performance of the digital equipment is characterized for error probabilities of $>10^{-4}$ to $<10^{-7}$. Broadband thermal noise is added to the modulated S-band signal just before the demodulator to simulate the required E_b/N_o range.

The BER of the equipment under test is determined by averaging the error rates of the I and Q channel. A sample data sheet is shown in Figure A-5, and the data is plotted on the form shown in Figure A-6. Several measurements over a period of several days are performed and the results averaged. This is done to eliminate any anomalous

45

data points. Using this technique, we have est. blished a measurement repeatability of better than ±0.3 dB for an error probability of 10^{-6}.

Configuration

Date

L.P.F.

$\frac{E_b}{N_o}$	Error Count		
	I Channel	Q Channel	Average

Figure A-5. Example Error Count Data Sheet

In addition to the BER data, time and frequency domain photographs are taken of the baseband, modulated, and demodulated signals as indicated in Table A-2. The photographs are analyzed to determine the transition time, asymmetry, and the spectrum occupancy of the signal.

3. LINK BIT ERROR RATE TESTING

Purpose: To determine the degration in digital terminal BER due to the distortion in the Ka-band wideband demonstration link.

Procedure: The basic procedure is to repeat all of the tests described in Section 2. The only difference is that the modulated signal is transmitted through the demonstration link prior to being demcdulated. In this way, the input and output data can be compared to determine the effects of the demonstration link for such factors as BER, risetime, asymmetry, and spectrum cccupancy.

46

Figure A-6. Example Bit Error Rate Curve

TABLE A-2. DIGITAL TESTING SUMMARY

Test Configuration	Data Recorded			Data Analysis			
	Error Count	Time Domain Photo	Frequency Domain Photo	Bit Error Rate	Transition Time	Asymmetry	Spectrum Occupancy
Data Generator Output		X			X	X	
QPSK Modulator Output			X				X
MSK Modulator Output			X				X
Coherent Demodulator	X	X		X	X	X	
Differentially Coherent Demodulator	X	X		X	X	X	

The link BER tests are performed both with and without the avalanche diode amplifier (refer to Figure A-2). In this way, the incremental degradation due to the output amplifier is evaluated. In addition, provision has been made to locate the band definition filter at either the modulator output or at the output of the downconverter. Complete testing is first performed with the filter located at the output of the downconverter (Figure A-2). The BER tests are then repeated with the filter placed at the output of the modulator. This test determines the effects of bandlimiting prior to the primary distortion elements in the transmitter vs filtering following these distortion elements.

MISSION
of
Rome Air Development Center

RADC plans and conducts research, exploratory and advanced development programs in command, control, and communications (C^3) activities, and in the C^3 areas of information sciences and intelligence. The principal technical mission areas are communications, electromagnetic guidance and control, surveillance of ground and aerospace objects, intelligence data collection and handling, information system technology, ionospheric propagation, solid state sciences, microwave physics and electronic reliability, maintainability and compatibility.